Chapter 1

Plane Electromagnetic Waves

LEARNING OBJECTIVES

- Develop and understand the spatial and temporal relationships between electric and magnetic fields for propagating waves
- Relate the spatial and temporal relationships between electric and magnetic fields for polarized waves
- Use dielectric, magnetic, and conduction properties of a medium to modify plane wave field properties
- Use the relative velocity between a source and receiver to find the relativistically accurate frequency shift (Doppler Shift) of harmonic E&M waves
- Recognize the difference between group and phase velocity and relate them to the transmission of power and transfer of momentum
- Describe the properties of plane waves that are incident on a boundary between two media with differing permittivity, permeability, and conductivity
- Show how E&M pulses attenuate and disperse in common transmission materials such as copper, glass, and liquids

INTRODUCTION

In the development of the solutions to Maxwell's equations (see Intent of the Book), we have used the scalar electric potential, $V(x, y, z, t)$, the magnetic vector potential, $\vec{A}(x, y, z, t)$, and the Lorenz gauge to uncouple the differential equations and to write an equivalent pair of inhomogeneous partial differential equations (PDEs) for V and $\vec{A}$:

$$\vec{\nabla}^2 V - \mu\varepsilon \frac{\partial^2 V}{\partial t^2} = -\frac{\rho_V}{\varepsilon} \tag{1.1a}$$

$$\vec{\nabla}^2 \vec{A} - \mu\varepsilon \frac{\partial^2 \vec{A}}{\partial t^2} = -\mu \vec{J} \tag{1.1b}$$

The Foundations of Signal Integrity, by Paul G. Huray

We have found that these PDEs can be solved independently to find a particular solution in terms of the time-harmonic source electric charge density, $\rho(x, y, z, t) = \rho_s(\vec{x})e^{j\omega t}$, and the source current density, $\vec{J}(x, y, z, t) = \vec{J}_s(\vec{x})e^{j\omega t}$, as

$$V(\vec{x}, \vec{x}', t) = \frac{1}{4\pi\varepsilon}\iiint_{V'} \frac{\rho_S(\vec{x}')e^{-jk|\vec{x}-\vec{x}'|}}{|\vec{x}-\vec{x}'|} d^3x' e^{j\omega t} \tag{1.2a}$$

$$\vec{A}(\vec{x}, \vec{x}', t) = \frac{\mu}{4\pi}\iiint_{V'} \frac{\vec{J}_S(\vec{x}')e^{-jk|\vec{x}-\vec{x}'|}}{|\vec{x}-\vec{x}'|} d^3x' e^{j\omega t} \tag{1.2b}$$

The most general form of the solution is then a linear combination of the general solutions to the homogeneous PDEs (Equation 1.1 in which $\rho = 0$ and $\vec{J} = 0$) and Equation 1.2. Knowing the relationship between electric field $\vec{E}(\vec{x}, t) = \vec{E}_S(\vec{x})e^{j\omega t}$ and magnetic field, $\vec{H}(\vec{x}, t) = \vec{H}_S(\vec{x})e^{j\omega t}$ and the scalar electric and magnetic vector potentials, we then develop an understanding of the behavior of those fields in a homogeneous material medium with electric permittivity, ε, electric conductivity, σ, and magnetic permeability, μ (where $\vec{B} = \mu\vec{H}$ and $\vec{D} = \varepsilon\vec{E}$):

$$\vec{H}_S = \frac{1}{\mu}\vec{\nabla}\times\vec{A}_S \tag{1.3a}$$

$$\vec{E}_S = -\vec{\nabla}V_S - j\omega\vec{A}_S \tag{1.3b}$$

These solutions satisfy the time-harmonic form of Maxwell's equations

$$\vec{\nabla}\times\vec{E}_S = -j\omega\mu\vec{H}_S \tag{1.4a}$$

$$\vec{\nabla}\times\vec{H}_S = \vec{J}_S + j\omega\varepsilon\vec{E}_S \tag{1.4b}$$

$$\vec{\nabla}\cdot\vec{E}_S = \frac{\rho_S}{\varepsilon} \tag{1.4c}$$

$$\vec{\nabla}\cdot\vec{H}_S = 0 \tag{1.4d}$$

so we are free to use these relationships where they are convenient. For example, if we use Equation 1.3a to find $\vec{H}_S$ in source-free space, we may use Equation 1.4b (in the absence of current density, $\vec{J}_S$) to find $\vec{E}_S$ without having to find V_s.

1.1 PROPAGATING PLANE WAVES

We begin by considering the propagation of a magnetic vector potential in a source-free region of space:

$$\vec{A}(\vec{x}, t) = \vec{A}_S(\vec{x})e^{j\omega t} = A_z^+(x, y)e^{-j(k_z z-\omega t)}\hat{a}_z + A_z^-(x, y)e^{j(k_z z+\omega t)}\hat{a}_z, \tag{1.5}$$

which is a linear combination of the two independent solutions to the homogeneous PDE 1.1b. Here, we have expressed the plane wave in terms of its motion along the

z-axis because we are at liberty to orient the Cartesian coordinates in a direction of our choice. By incrementing the time t in this expression from t' to $t' + dt$, we can follow a point of constant phase, $(k_z z - \omega t) = \text{constant}$, to see that the first term represents the propagation of a wave in the z-direction (along the positive z-axis), with speed $u_p = dz/dt = \omega/k_z = 1/\sqrt{\mu\varepsilon}$ (also called the phase velocity). The second term in Equation 1.5 represents the propagation of a wave along the negative z-axis with the same phase velocity. To simplify our understanding of the wave propagation and the relative position of the resulting electric and magnetic fields, we will assume that the boundary conditions require the coefficient of the second term to be zero; that is, we will consider only propagation in the positive z-direction. Such a field might, for example, be created by current sources in a region of space in which the electric current density is forced by boundary conditions to have a component only in the z-direction.

Relative Directions and Magnitudes of $\vec{E}$ and $\vec{H}$

For the special case with $A_z^-(x, y) = 0$, we can use Equation 1.3a to see that

$$\vec{H}_S^+ = \frac{1}{\mu}\vec{\nabla}\times\vec{A}_S^+ = \frac{1}{\mu}\begin{vmatrix} \hat{a}_x & \hat{a}_y & \hat{a}_z \\ \dfrac{\partial}{\partial x} & \dfrac{\partial}{\partial y} & \dfrac{\partial}{\partial z} \\ 0 & 0 & A_z^+(x,y)e^{-jk_z z} \end{vmatrix}$$
$$= \frac{1}{\mu}\frac{\partial A_z^+}{\partial y}e^{-jk_z z}\hat{a}_x - \frac{1}{\mu}\frac{\partial A_z^+}{\partial x}e^{-jk_z z}\hat{a}_y \tag{1.6a}$$

We can also use Equation 1.4b to see that

$$\vec{E}_S^+ = \frac{1}{j\omega\varepsilon}\vec{\nabla}\times\vec{H}_S^+ = \frac{1}{j\omega\varepsilon\mu}\begin{vmatrix} \hat{a}_x & \hat{a}_y & \hat{a}_z \\ \dfrac{\partial}{\partial x} & \dfrac{\partial}{\partial y} & \dfrac{\partial}{\partial z} \\ \dfrac{\partial A_z^+}{\partial y}e^{-jk_z z} & -\dfrac{\partial A_z^+}{\partial x}e^{-jk_z z} & 0 \end{vmatrix}$$
$$= \frac{1}{j\omega\varepsilon\mu}\frac{\partial^2\left(A_z^+e^{-jk_z z}\right)}{\partial x\partial z}\hat{a}_x + \frac{1}{j\omega\varepsilon\mu}\frac{\partial^2\left(A_z^+e^{-jk_z z}\right)}{\partial y\partial z}\hat{a}_y$$
$$= \frac{-k_z}{\omega\varepsilon\mu}\frac{\partial A_z^+}{\partial x}e^{-jk_z z}\hat{a}_x + \frac{-k_z}{\omega\varepsilon\mu}\frac{\partial A_z^+}{\partial y}e^{-jk_z z}\hat{a}_y \tag{1.6b}$$

We may now see that

$$\vec{H}_S^+ \cdot \vec{A}_S^+ = 0 \tag{1.7a}$$
$$\vec{E}_S^+ \cdot \vec{A}_S^+ = 0 \tag{1.7b}$$
$$\vec{H}_S^+ \cdot \vec{E}_S^+ = 0 \tag{1.7c}$$

Conclusion

In this special case, the propagating electric field intensity waves, magnetic field intensity waves, and magnetic vector potential waves are all orthogonal to one another. We call such propagating waves transverse electric (TE^z) and transverse magnetic (TM^z) because they are moving in the z-direction, in phase with the magnetic vector potential. When both TE and TM waves occur in the same propagation (as they do here), the waves are transverse electromagnetic and labeled TEM^z waves.

Relative Magnitudes

We can also use the relationship $k_z = \omega\sqrt{\mu\varepsilon}$ to compare the components of the electric and magnetic field intensity for TEM^z waves as

$$\frac{E^+_{S,x}}{H^+_{S,y}} = \sqrt{\frac{\mu}{\varepsilon}} = Z^+_W = \eta \tag{1.8a}$$

$$-\frac{E^+_{S,y}}{H^+_{S,x}} = \sqrt{\frac{\mu}{\varepsilon}} = Z^+_W = \eta \tag{1.8b}$$

The quantity η is called the ***intrinsic impedance*** of the medium because it is a function only of the permeability and permittivity of the medium. Some texts call this ratio, Z_W, which they call the ***wave impedance***, to remind us that the ratio of an electric field intensity and magnetic field intensity has units of ohms. Thus, this quantity is a measure of the impedance of the medium; the ratio is labeled Z_0 in the case of waves propagating in a vacuum. In air or a vacuum, $\varepsilon = \varepsilon_0 \approx (1/36\pi) \times 10^{-9}$ F/m or (s/Ωm) and $\mu = \mu_0 = 4\pi \times 10^{-7}$H/m or (Ωs/m) so $\eta = Z_0 \approx 120\pi\Omega = 377\Omega$. This is called the ***intrinsic impedance of free space***.

Physical Meaning of the Propagating Wave Equations

Equations 1.6 give us the relative vector directions, phase, and magnitude of $\vec{E}$ and $\vec{H}$ relative to the magnetic vector potential, $\vec{A}$. Without some knowledge of how $\vec{A}$ varies with x and y, we cannot take the partial derivatives. However, the x-direction is just as arbitrary as the z-direction, which we choose to be in the direction of propagation of $\vec{A}$. We can therefore choose the x-direction to be in the direction of the electric field intensity vector, in which case, we write

$$\vec{E}^+(\vec{x}, t) = E^+_0 e^{-j(k_z z - \omega t)} \hat{a}_x \tag{1.9a}$$

$$\vec{H}^+(\vec{x}, t) = \left(E^+_0 / \eta\right) e^{-j(k_z z - \omega t)} \hat{a}_y \tag{1.9b}$$

Here, we have chosen the component of $\vec{H}$ to satisfy the ratio condition required by Equation 1.8a.

Assuming the coefficient in 1.9a is a real number, let us now diagram the propagating waves for the real part of the functions 1.9:

$$\mathrm{Re}\left[\vec{E}^{+}(\vec{x},t)\right]=E_0^{+}\cos(k_z z-\omega t)\hat{a}_x \tag{1.10a}$$

$$\mathrm{Re}\left[\vec{H}^{+}(\vec{x},t)\right]=\left(E_0^{+}/\eta\right)\cos(k_z z-\omega t)\hat{a}_y \tag{1.10b}$$

A graph of these functions is shown in Figure 1.1 at time $t = 0$.

In Figure 1.1, we see that, at time $t = 0$, both the electric field intensity and the magnetic field intensity are distributed under a cosine curve envelope in space with a wavelength $\lambda = 2\pi/k_z$ and both envelopes are propagating along the positive z-axis with velocity $u_p = \lambda f = 1/\sqrt{\mu\varepsilon}$.

In this figure, the x-axis direction has been chosen to lie in the direction of the electric field, and Equations 1.7 thus require that the magnetic field must lie in the y-direction. We may use the right-hand rule to see that $\vec{E}\times\vec{H}$ lies in the direction of $\vec{A}$ (the z-direction) at every point in space. Furthermore, the electric field intensity and the magnetic field intensity remain in phase with one another (both are a maximum at the same point in space and both are zero at the same point). For later values of time, both continue to point in their respective x- and y-directions so we say that they are linearly polarized. Finally, we note that the magnitude of the magnetic field envelope $H_0^{+} = E_0^{+}/\eta$, where E_0^{+} is the magnitude of the electric field intensity envelope and $\eta = \sqrt{\mu/\varepsilon}$ is the intrinsic impedance of the medium in which the wave is propagating.

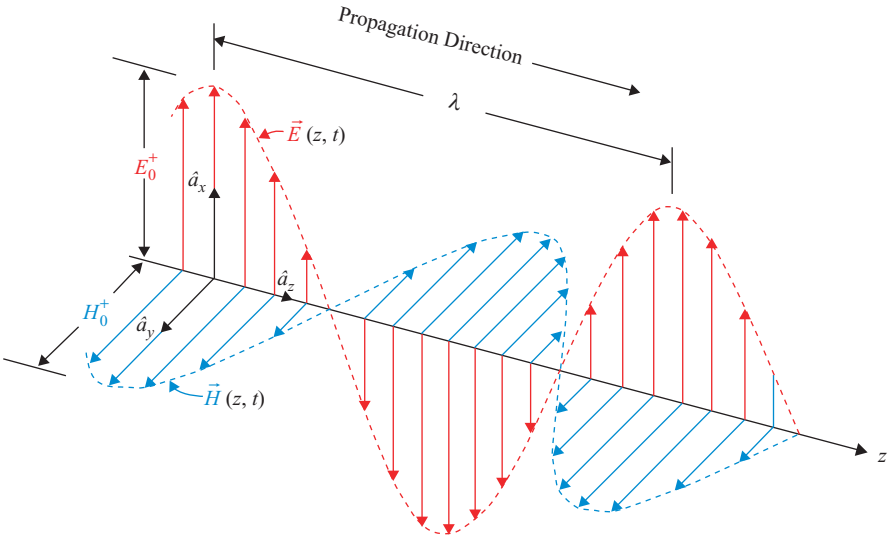

Figure 1.1 Plot of the real parts of the electric and magnetic field intensity as a function of position z, at time $t = 0$ when the x-axis is chosen to lie in the direction of the electric field intensity vector.

NOTE Some texts prefer to graph the magnetic flux density $\vec{B} = \mu\vec{H}$ rather than the magnetic field intensity

$$B_0^+ = \mu\sqrt{\frac{\varepsilon}{\mu}}E_0^+ = \sqrt{\mu\varepsilon}\,E_0^+ = \frac{E_0^+}{u_P} \tag{1.11}$$

because, in the ***special case*** when the propagating medium (e.g., air) has the same permeability and permittivity of free space, $B_0^+ = E_0^+/c$, where c is the speed of light in a vacuum, 2.99792458×10^8 m/s. When the electric field intensity of an electromagnetic wave remains in the same direction as it propagates in a medium, it is said to be linearly polarized. Of course, the relations above show that the magnetic field intensity associated with the wave is also linearly polarized.

1.2 POLARIZED PLANE WAVES

An observer located along the z-axis at a position of maximum electric field (i.e., at position $z = n\lambda$ with n = an integer at $t = 0$) looking back in the $-z$ direction (as shown in Figure 1.2a) would see the electric and magnetic field intensity, as shown in Figure 1.2b.

As a function of time, an observer at $z = n\lambda$ would measure the electric field intensity to be a maximum (in the x-direction) at time $t = 0$, as shown in Figure 1.2b, then observe it to decrease to zero by time $t = (1/4)(\lambda/c)$, then observe it to further decrease to its maximum negative value by time $t = (1/2)(\lambda/c)$, then increase back to zero by $t = (3/4)(\lambda/c)$, then increase back to its maximum positive value by $t = \lambda/c$, and so forth in a cosinusoidal manner with time. The magnetic field intensity

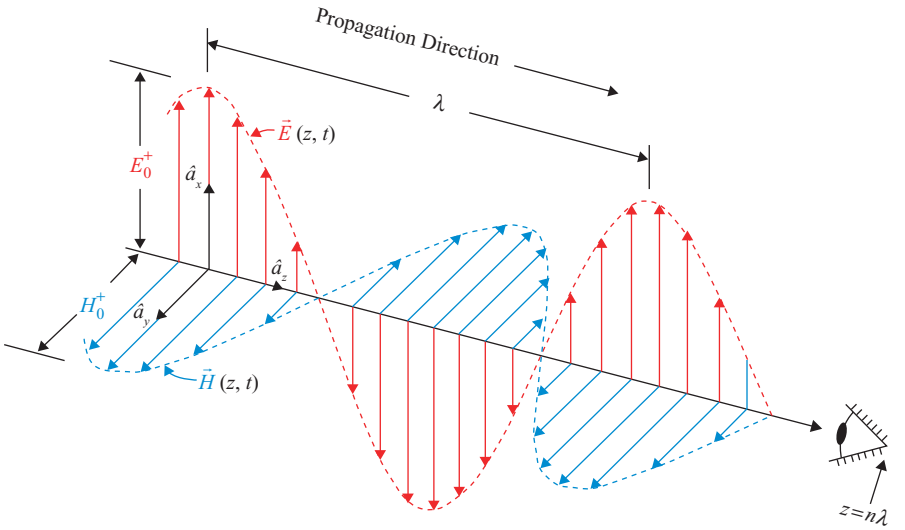

Figure 1.2 (a) Observer at $z = n\lambda$ (n = integer);

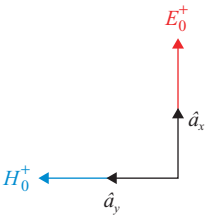

Figure 1.2 (b) electric and magnetic field intensity components observed at time $t = 0$.

would be behaving in a similar manner except it would occur only in the y-direction, and its amplitude would be $H_0^+ = E_0^+/\eta$.

More General Case

If we express the field intensity in the general case (not choosing the x-axis to lie in the direction of the electric field intensity), Equations 1.6a and 1.6b specify their components:

$$\vec{E}_S^+(z) = \frac{-k_z}{\omega\varepsilon\mu}\frac{\partial A_z^+}{\partial x}e^{-jk_z z}\hat{a}_x + \frac{-k_z}{\omega\varepsilon\mu}\frac{\partial A_z^+}{\partial y}e^{-jk_z z}\hat{a}_y$$
$$\vec{E}^+(z,t) = E_{0,x}^+ e^{-j(k_z z-\omega t)}\hat{a}_x + E_{0,y}^+ e^{-j(k_z z-\omega t)}\hat{a}_y \quad (1.12a)$$

$$\vec{H}_S^+(z) = \frac{1}{\mu}\frac{\partial A_z^+}{\partial y}e^{-jk_z z}\hat{a}_x - \frac{1}{\mu}\frac{\partial A_z^+}{\partial x}e^{-jk_z z}\hat{a}_y$$
$$\vec{H}^+(z,t) = H_{0,x}^+ e^{-j(k_z z-\omega t)}\hat{a}_x + H_{0,y}^+ e^{-j(k_z z-\omega t)}\hat{a}_y, \quad (1.12b)$$

where the components of $\vec{E}$ and $\vec{H}$ obey the relations 1.8a and 1.8b, $E_{0,x}^+ = H_{0,y}^+ = \eta$, and $E_{0,y}^+/H_{0,x}^+ = -\eta$. In this case, we can draw the electric field measured by the observer at position $z = n\lambda$ (n = integer) at time $t = 0$ to be that shown in Figure 1.3.

As seen from a point $z = n\lambda$ on the z-axis, the two components of electric field would add vectorally to form a resultant vector $\vec{E}_{0,R}^+$ whose components would vary with time cosinusoidally. Thus, $\vec{E}_{0,R}^+$ would be seen as a linearly polarized field at angle

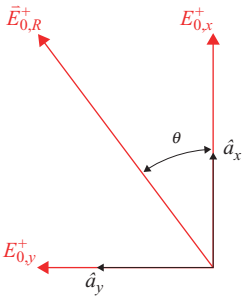

Figure 1.3 Components of the electric field intensity observed at time $t = 0$ (components of the magnetic field intensity are orthogonal to these components but are not shown).

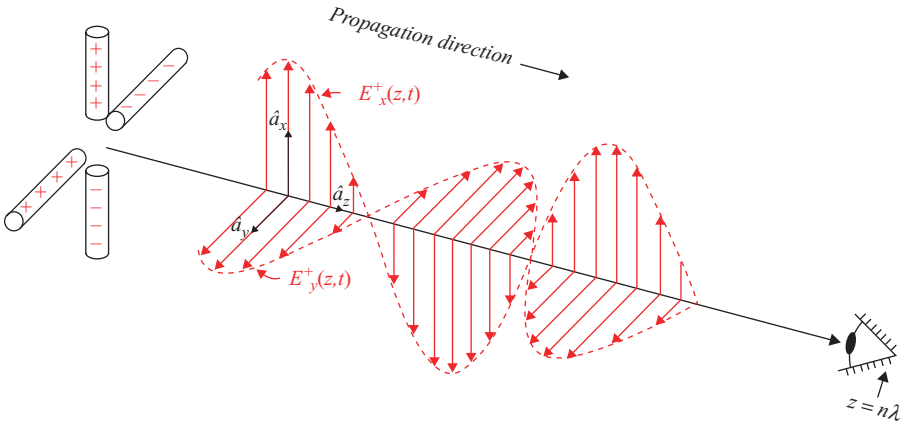

Figure 1.4 Two electric field intensities produced by orthogonal dipole antennas operating at the same frequency and with the same phase.

$$\theta = \tan^{-1}\left(E^+_{0,y} \big/ E^+_{0,x}\right) \tag{1.13}$$

with respect to the x-axis. We would say that the two components of the electric field are in ***space quadrature*** with one another. While both of the measured components change with time in a $\cos\omega t$ manner, the angle θ remains constant so the resultant polarized electric field oscillates in amplitude with the same orientation with respect to the x-axis.

A simple way to picture the resultant of two components is to picture them as originating from two orthogonal sources such as the two dipole antennas shown in Figure 1.4.

Even More General Case

If the two dipole antennas that create the two space quadrature polarized electric field intensities are displaced from one another along the z-axis by an amount $z = \lambda/4$, as shown in Figure 1.5 and are driven at the same frequency and in the same phase, the resulting electric field intensities will be *displaced from one another in phase* by one quarter of a cycle. As seen by the observer at $z = n\lambda$, the second electric field intensity (oriented in the y-direction) will be delayed in time from the first (oriented in the x-direction) by $t = (\pi/2)/\omega$.

The equivalent equation for the observed electric fields at point z is

$$\mathrm{Re}\left[\vec{E}^+_S(z,t)\right] = \mathrm{Re}\left[E^+_{0,x}e^{-j(k_z z-\omega t)}\hat{a}_x + E^+_{0,y}e^{-j\left(k_z z-\omega t-\frac{\pi}{2}\right)}\hat{a}_y\right] \quad \text{or} \tag{1.14}$$

$$\begin{aligned}\mathrm{Re}\left[\vec{E}^+_S(z,t)\right] &= E^+_{0,x}\cos(k_z z-\omega t)\hat{a}_x + E^+_{0,y}\cos\left(k_z z-\omega t+\frac{\pi}{2}\right)\hat{a}_y \\ &= E^+_{0,x}\cos(k_z z-\omega t)\hat{a}_x - E^+_{0,y}\sin(k_z z-\omega t)\hat{a}_y\end{aligned} \tag{1.15}$$

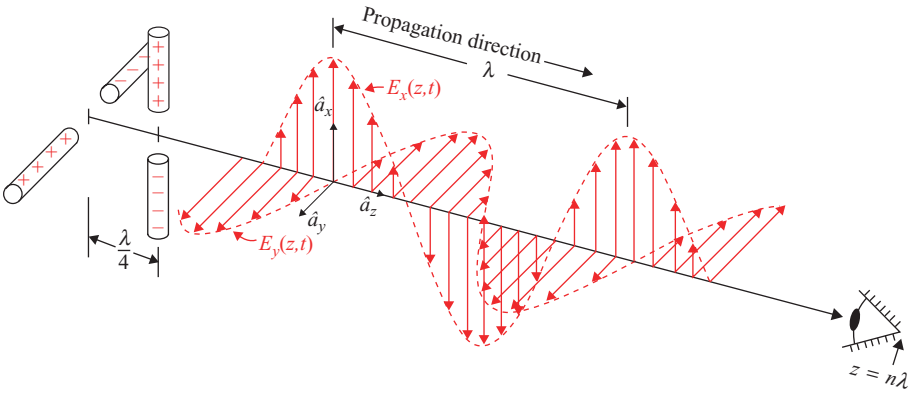

Figure 1.5 Polarized electric field intensities in space and time quadrature.

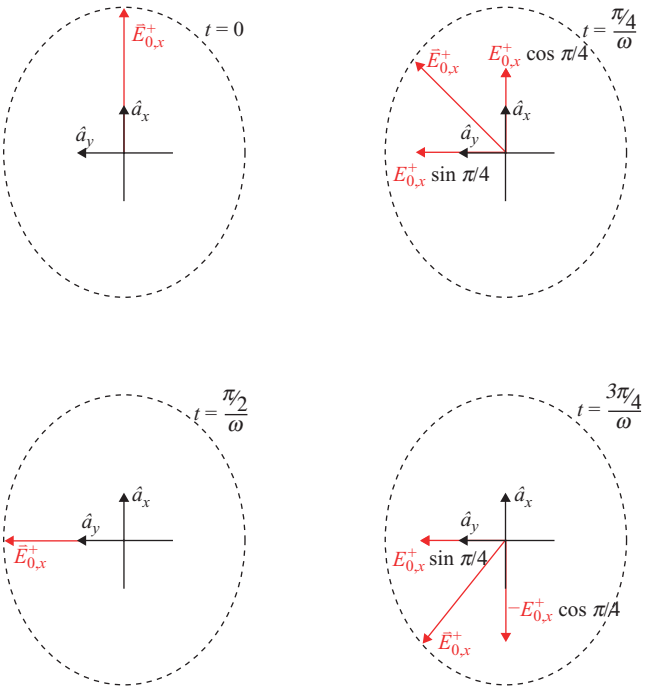

Figure 1.6 Vector sum of the electric field intensities produced by two sources, one of which lags the other by $\pi/2$.

If we plot these terms for $z = n\lambda$ on a graph like that shown in Figure 1.3 for a sequence of times, we get the sequence shown in Figure 1.6.

We can see from the resultant vector in Figure 1.6 that $\vec{E}_R$ rotates in a counterclockwise manner about the origin, with radial frequency ω, and traces out the path

of an ellipse in time as the wave propagates along the z-axis. Such resultant electromagnetic waves are called ***right-hand elliptically polarized*** waves.

Similarly, we can see that, if the component of the electric field intensity in the y-direction leads the component in the x-direction by $t = (\pi/2)/\omega$, the result will be ***left-hand elliptically polarized*** waves.

1.3 DOPPLER SHIFT

Each evening, the news channel brings us the local Doppler radar map of weather in our area, the police track our automobile speed with Doppler laser reflection, the universe is said to be expanding because we can observe and measure the "Red Shift" of stars, scientists use Mössbauer measurements to determine the magnetic flux density at a nucleus, and a trip to a NASCAR event is made more exciting by the change in pitch of a car engine as it zooms past us in the stands. A physician may take a Doppler angiogram movie of a beating heart, or an ultrasound technician may make pictures of a moving fetus in a womb. These events, as well as some troublesome problems such as the change in frequency of a mobile cell phone as measured by a base station, are caused by the motion of a source of waves relative to a receiver.

We can understand the phenomenon of Doppler shift by considering the change in waves produced by a stationary source of electromagnetic waves as it differs from a source in motion with constant velocity, as shown in Figure 1.7.

Suppose a source of electromagnetic waves (such as a quasar) produces TEM^r waves, with period Δt_0 between the crests of electric field intensity. These waves move in the z-direction, with velocity c toward an observer at rest with respect to the source, as shown in the top sketch in Figure 1.7. The distance between the crests (the wavelength) is then $\lambda_0 = c\Delta t = c\Delta t_0$.

Now, let us view that same source of electromagnetic waves as it moves away from the observer at velocity, v. Because the source is moving with respect to the observer, there will be a change in the period of the source that follows time dilation, according to the special theory of relativity:

$$\Delta t = \frac{\Delta t_0}{\sqrt{1 - v^2/c^2}} \tag{1.16}$$

Now, the distance between crests of the electric field intensity will be

$$\lambda = c\,\Delta t + v\,\Delta t = \frac{(c+v)\,\Delta t_0}{\sqrt{1 - v^2/c^2}} = c\,\Delta t_0 \frac{(1+v/c)}{\sqrt{(1+v/c)(1-v/c)}} = \lambda_0 \sqrt{\frac{(1+v/c)}{(1-v/c)}} \tag{1.17}$$

Because the speed of light, c, is the same for all observers,

$$f = \frac{c}{\lambda} = \frac{c}{\lambda_0}\sqrt{\frac{(1-v/c)}{(1+v/c)}} = f_0\sqrt{\frac{(1-v/c)}{(1+v/c)}} \tag{1.18}$$

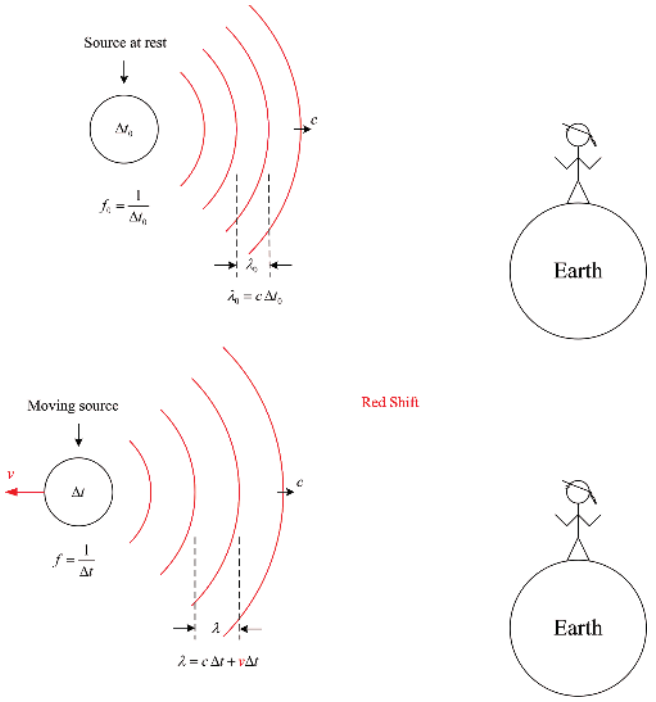

Figure 1.7 Change in the frequency and wavelength of electromagnetic waves from a source at rest versus a source moving at velocity v relative to the observer. Here, the crest (highest intensity) of the transverse electric field waves is shown as outward expanding circles about their source.

Equation 1.18 is the ***Doppler equation*** for the frequency of a moving source relative to a stationary observer. Equation 1.18 is often written in its series form

$$\frac{f}{f_0} = \left[1 - \frac{v}{c} + \frac{1}{2}\frac{v^2}{c^2} - \frac{1}{2}\frac{v^3}{c^3} + \cdots\right] \tag{1.19}$$

because the velocity of the source is normally much less than the speed of light, so we can make a good approximation to the size of the Doppler shift by keeping only the first two terms in Equation 1.19.

However, one theory of quasars is that they were expelled in the "Big Bang" at tremendous velocities; some close to the speed of light. For these sources of electromagnetic waves, we can write an expression for the relative shift in wavelength as

$$Z = \frac{\lambda - \lambda_0}{\lambda_0} = \sqrt{\frac{(1+v/c)}{(1-v/c)}} - 1 \tag{1.20}$$

Table 1.1 Values of relative wavelength shift and corresponding value of velocity relative to the speed of light for several stellar objects

Stellar object	Z	v/c
Quasar QSO (0H471)	3.4	0.90
Quasar 4C (05.34)	2.88	0.88
AO 0235 + 164 (Mg at 2800 Å)	0.52392	0.398
AO 0235 + 164 (H at 21 cm)	0.52385	0.398
Galaxy with the largest Z	0.46	0.36

The quantity Z has been measured for a number of stellar objects as listed in Table 1.1: Many astronomers have concluded that the consistency of measurements of relative wavelength shifts from several spectra (such as hydrogen and mercury) confirms the Doppler effect to be responsible for the red shift of electromagnetic waves from stellar objects.

Intensity Dilemma

Suppose a quasar of radius r_0 has a luminosity, I_0, at its surface, as shown in Figure 1.8.

Measurements show quasistellar object QSO 3C466 varies in brightness by a factor of *2* in 1 day (i.e., its radius must be less than 1 light-day $\approx 2.7 \times 10^{13}$ m), its red shift gives a velocity of 0.90 c, and its luminosity is about $I \approx 10^{22}$ erg/s. If the object has been traveling at this speed since the Big Bang ($\approx \pi \times 10^{17}$ s), by now it

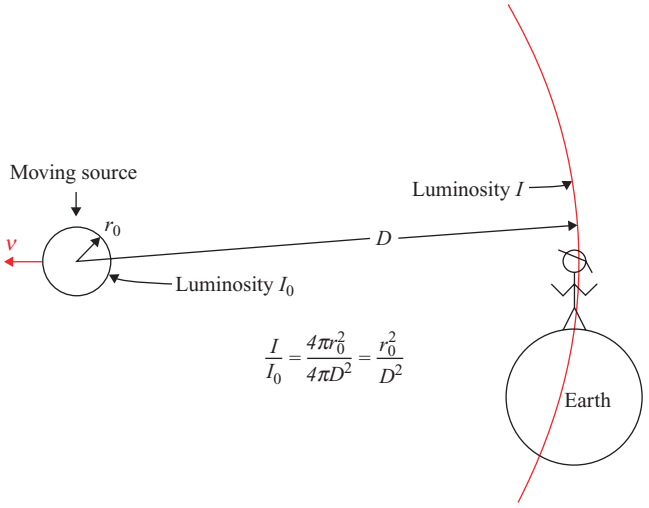

Figure 1.8 Observed luminosity (power density) of electromagnetic waves from a quasistellar object at distance D.

must be $D \approx 0.9 \times 3 \times 10^8 \times 3.14 \times 10^{17}$ m $= 8.5 \times 10^{25}$ m away from the center of the universe. Using its observed luminosity, we calculated that the luminosity at its surface (at a distant point in time) must have been at least $I_0 \approx 10^{47}$ erg/s. The luminosity of our sun is about 10^{33} erg/s. How massive would a quasar have to be to produce an intensity 10^{14} times larger than that of our sun? Would not that mass have collapsed into a black hole?

Herman Weyl Solution?

Could it be that the observed shift in frequency is not a result of a Doppler shift but of some other mechanism? For example, in 1918, Hermann Weyl suggested that there might be a frequency shift of clocks that is proportional to their electromagnetic history (i.e., the magnetic flux they have enclosed, (BA), or equivalently, their electric potential, V, in a period of time, Δt: $\Delta f_{Quasar}/f_0 \cong -Z/(Z+1) = 0.47 = C_{HW}/e(BA)$ *or* $C_{HW}c/e(V\Delta t)$. Thus, for a quasar at electric potential of 10^8 V (according to Schwartzman, the theoretical maximum that will not blow a quasar apart) for all of time ($\pi \times 10^{17}$ s), we would expect a dimensionless Herman Weyl constant, C_{HW}, of about 10^{-43}. If this were the explanation of the observed frequency shift, the quasars would not be traveling away at such a high velocity but would have had their frequencies shifted by the Herman Weyl effect. Would it be possible to measure such a small constant in a laboratory? The author and others made such a measurement by using the Mössbauer effect and showed[1] that the Herman Weyl coefficient (if it exists at all) is at most $\pm 2 \times 10^{-48}$. One of the beautiful aspects of science is that answers to phenomenon often lead to other unanswered questions. The issue of low intensity of light from quasars today remains unanswered to many scientists' satisfaction.

We have seen that the Doppler shift adequately explains the frequency shift of electromagnetic waves with frequencies in the visible spectrum (10^{15} Hz), even for relative velocities that approach the speed of light, $c = 3 \times 10^8$ m/s. We have also personally observed that the Doppler shift explains the modulation in audible frequencies (10^2–10^5 Hz) for automobiles or trains traveling at relative velocities of 10^3–10^5 m/s. The National Aeronautics and Space Administration (NASA) had a Doppler effect scare on a mission to Titan that almost resulted in mission failure.

The NASA Cassini Example

In 2005, NASA had a mission to Saturn's moon, Titan, that used an orbiter named Cassini to receive communications from a probe named Huygens as it fell to the surface of Titan at a terminal velocity of 5.5 km/s.

Sample Calculation

The Doppler shift observed by Cassini was 38 kHz when it was directly overhead the falling Huygens probe. We can thus find the base carrier frequency sent by the

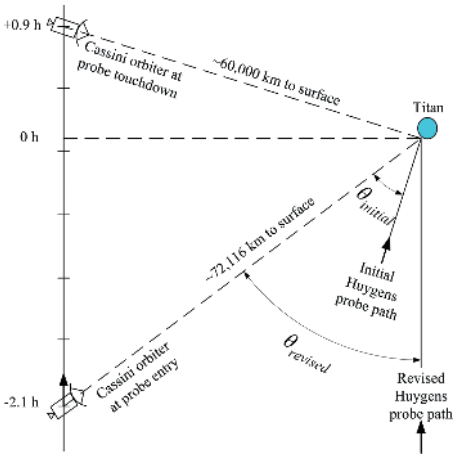

Figure 1.9 Revised position of the Cassini Orbiter relative to the Huygens Probe during entry (and transmission of pictures) to minimize the relative component of velocity, $v\cos\theta$, between transmitter and receiver.

probe by writing the Doppler equation in its series form $f/f_0 = [1 - v/c + (1/2)v^2/c^2 - (1/2)v^3/c^3 + \cdots]$, or $f/f_0 \approx [1 - v/c]$ if the velocity of the source is much less than the speed of light. Thus, the frequency shift $\Delta f \approx f - f_0 = [1 - v/c]\, f_0 - f_0 = -(v/c)f_0$ and for $\Delta f = -38$ kHz, $f_0 \approx (3 \times 10^8$ m/s$/5.5 \times 10^3$ m/s) (38 kHz) = 2.07 GHz.

NASA engineers solved the problem by launching the Huygens probe on the third (rather than the second) orbit about Saturn so that the Cassini receivers were moving nearly perpendicular to the probe decent (thus reducing the relative speed, v, to $v\cos\theta$ between the transmitter and the receiver). This change in relative motion reduced the Doppler shift to the point that the Cassini receivers would not loose lock on the carrier frequency. Figure 1.9 shows the revised location of the Cassini Orbiter as it began to communicate with the Huygens Probe during its descent onto Titan.

PROBLEMS

1.1 With the aid of drawings, explain what happened to the frequency of the signals received by the Cassini orbiter as it moved to an angle $\theta_{revised}$ relative to the path of the falling Huygens probe (assuming it was falling at its terminal velocity). Hint: The effect of time dilation is still valid when perpendicular relative motion is involved.

1.2 Calculate the Doppler shift of a 1.8 GHz cell phone due to its motion in a moving automobile at 70 mph if it is traveling (a) toward or (b) away from a Base Station.

The Mössbauer effect has been used to show that the Doppler shift also works for frequencies of 10^{19} Hz and for velocities as low as 10^{-5} m/s. The following section gives an example of the Mössbauer effect for ^{57}Fe nuclei and shows that the Doppler shift is so precise that it can be used to explain high-Q nuclear linewidths.

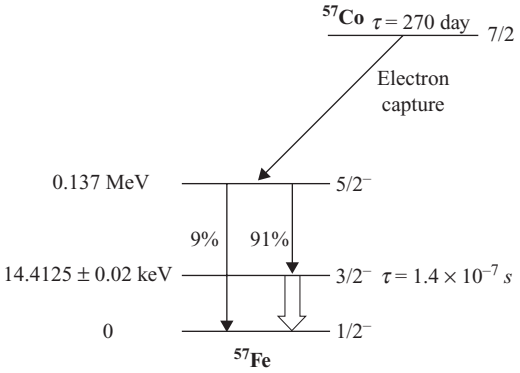

Figure 1.10 Nuclear energy levels of a ^{57}Fe nucleus following its population from the electron capture of a ^{57}Co nucleus (Table of Isotopes).

The Mössbauer Effect Example

When ^{57}Co captures an electron, it populates the 14.4125 keV excited state of ^{57}Fe (with a 98 ns half-life or lifetime $\tau = 1.4 \times 10^{-7}$ s), as shown in Figure 1.10.

The nuclear angular momentum quantum number of the excited state is $^3/_2$ and that of the ground state is $^1/_2$. Thus, in the absence of a magnetic field intensity at the ^{57}Fe nucleus, there are mono-energetic γ-rays emitted, with an energy of 14.4125 keV.* Mössbauer showed that these γ-rays are predominantly emitted in a nearly recoilless fashion because the ^{57}Fe nuclei are in a crystal lattice of mass $M = N_A \times m_{Fe}$ absorbs the momentum of the outgoing γ-ray. The frequency of the emitted γ-rays is thus $f_\gamma = 14.4125 \times 10^3$ eV/4.13566727 $\times 10^{-15}$ eV = 3.484227×10^{18} Hz. When γ-rays of this frequency impinge upon ^{57}Fe nuclei in a target material, as shown in Figure 1.11, they are often absorbed by those nuclei and later reemitted in a random direction. Thus, a detector behind the target will see a reduced number of γ-rays when there is absorption (at the resonant frequency).

By moving the source of nuclei (just like the quasar) away from the absorber at a velocity of $v = 0.3$ mm/s, we can Doppler shift their frequencies by a very small amount $v/c = 0.3$ mm/s/3×10^8 m/s = 10^{-12} (a vanishingly small amount compared with the frequency shift of a quasar), as shown in Figure 1.11.

As we see in Figure 1.12, this small Doppler shift is sufficient to completely take the γ-rays out of resonance so that the detector sees less absorption (the count rate goes up). This is called a Mössbauer effect absorption spectrum.

If the absorber nuclei experience a magnetic flux density, $\vec{B}$, then the excited and ground states of the absorber split into energy levels according to the Zeeman effect, $U_e = -\vec{\mu}_e \cdot \vec{B}_e$, where $\vec{\mu}_e$ is the nuclear magnetic moment of the nucleus in its excited state and $U_g = -\vec{\mu}_g \cdot \vec{B}_g$, where $\vec{\mu}_g$ is the nuclear magnetic moment of the nucleus in its ground state. The effect of the splitting is shown schematically in

*The energy of the 98 ns ^{57}Fe γ-ray is given here to 6 decimal places (our ability to measure it) but the nucleus knows this energy to about 15 decimal places as is shown below.

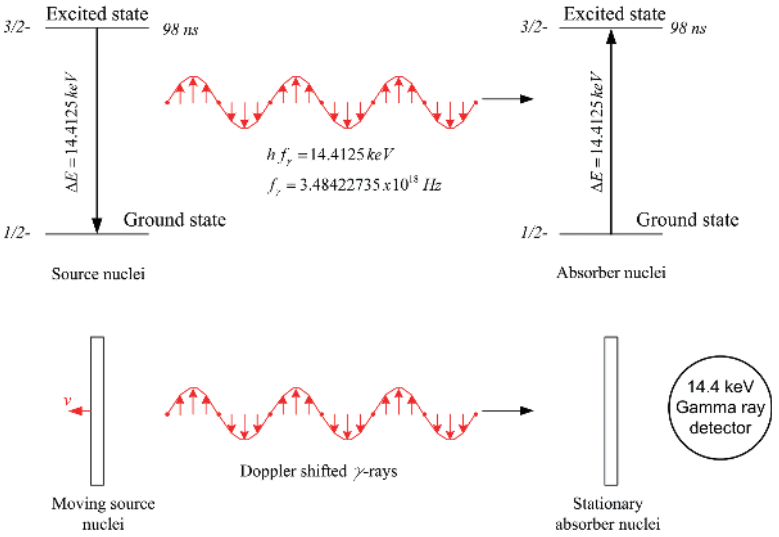

Figure 1.11 Gamma ray emission and absorption scheme for recoilless ^{57}Fe nuclei and a mechanism for shifting their frequency by a Doppler velocity of the emitted nuclei.

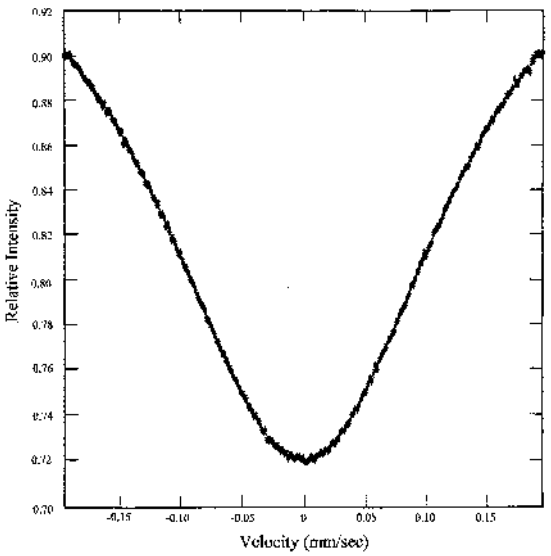

Figure 1.12 14.4125 keV γ-ray counts detected as a function of the Doppler velocity of the source for a non-magnetic source and a non-magnetic absorber.

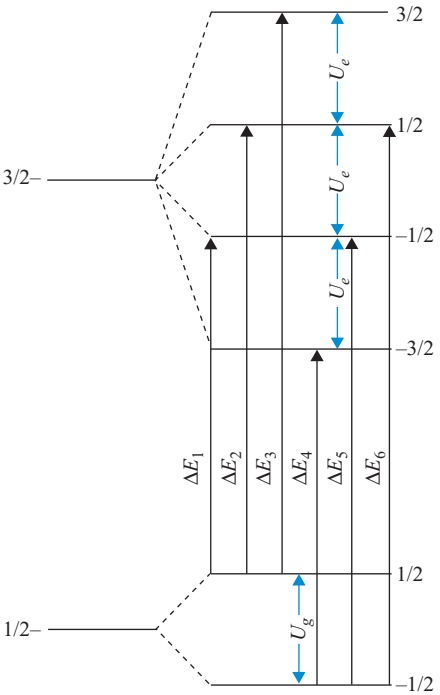

Figure 1.13 Energy splitting of the nuclear states of ^{57}Fe absorber nuclei brought about by Zeeman energy shifts for nuclei with magnetic moment in magnetic flux density.

Figure 1.13. Here, the splitting is *greatly exaggerated* as compared with the energy of the incident γ-rays.

Because the angular momentum of the incident γ-rays is 0 or $\pm 1\ \hbar\omega$ (depending upon whether the photon is linearly, right, or left circularly polarized), the transition between an absorber $-\frac{1}{2}$ ground state to a $+\frac{3}{2}$ excited state (or a $+\frac{1}{2}$ ground state to a $-\frac{3}{2}$ excited state) is not possible; it is said to be a forbidden transition. Thus, there are only six different energies that the incident γ-rays can have that will be absorbed (as shown in the schematic of Figure 1.13). We would thus expect six different Doppler velocities for which Mössbauer absorption will occur. A typical absorption spectrum of a nonmagnetic ^{57}Fe source with a magnetic ^{57}Fe absorber is shown in Figure 1.14.

The Mössbauer absorption spectrum gives us a way to measure the magnetic flux density at absorber nuclei. The energy levels and the distribution of the intensity levels can be strongly dependent on the neighboring atoms to the absorber nuclei. In many cases, a Mössbauer absorption spectrum can give us qualitative and quantitative measures of the atomic structure of an otherwise unknown sample and they can give us the values of magnetic field intensity and electric field gradient at the nuclei of atoms (a subatomic effect we normally ignore in our macroscopic treatment of electromagnetic fields). This effect is the subject of a whole class of experimental studies.

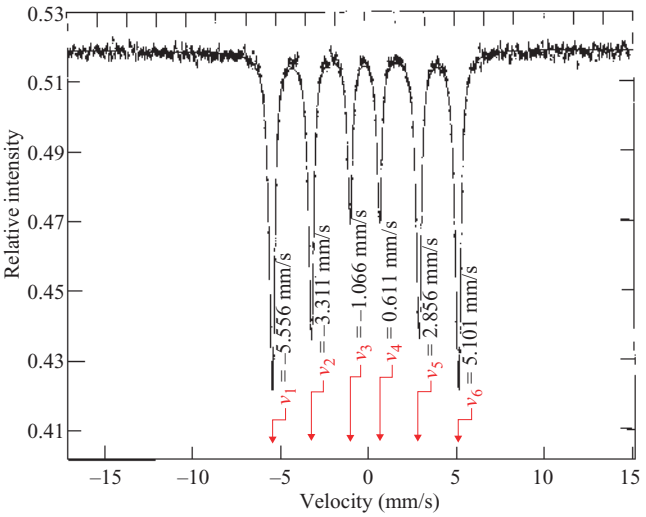

Figure 1.14 Mössbauer spectrum of a nonmagnetic ^{57}Fe source and a magnetic ^{57}Fe absorber.

Using the Doppler shift in the Heisenberg uncertainty principle, $\Delta E_{1/2}\Delta t_{1/2} \geq \hbar/2$ gives $(\Delta v_{1/2}/c)(E_\gamma)\Delta t_{1/2} \geq \hbar/2$ as the uncertainty for the Doppler velocity of the nuclear decay and absorption process. For a 14.4125 keV gamma ray with a half-life of 98 ns, we find $\Delta v_{1/2} \geq 0.07$ mm/s for the source nuclei and the same for the absorber nuclei for an expected uncertainty (Half Width at Half Max [HWHM]) of any of the Mössbauer absorption peaks of 0.14 mm/s, which compares well with the absorption peaks in Figure 1.12 or 1.14.

Conclusion

The uncertainty in the Doppler velocity for a nuclear decay and absorption process is limited only by the Heisenberg uncertainty principle. We that conclude the absorbing nuclei know the resonant energy of the emitted gamma rays at 3.5×10^{18} Hz to a precision of better than 10^{-13}.

Unified Field Theory Application

Gravitational Potential

The precision of the Mössbauer effect was one of its characteristics that permitted a measurement[2] to verify Einstein's principle of equivalence regarding gravitation and space-time. Einstein postulated that, in an enclosed elevator, it would be impossible to distinguish between a force due to a gravitating body like the earth (which caused a weight on a scale) and that due to an upward accelerating elevator. Because acceleration gave the same result as a force, he said that it was equivalent to invoke

either a linear space-time with an additional force due to gravity or a curvature in space near a gravitating body with no additional gravitational forces. An experimental test of this equivalence was given by Eddington and Dyson, who observed an eclipse of May 29, 1919, on the islands of Sobral (off Brazil) and Principe (in the Gulf of Guinea). They observed the light from a star that passed behind the sun at the instant of eclipse to continue to be visible as a result of the apparent curvature of space around the sun by an angle of 1.8 s of arc.[3] A simple explanation of the equivalence is that this would be the equivalent deflection of a photon with effective mass $m_{photon} = E_{photon}/c^2 = hf/c^2$ as it passed by the enormous mass of the sun (in this case, f is the frequency of visible light [~10^{15} Hz]).

However, it was 40 years before a test of the time component of space-time curvature could be measured. This part of the principle of equivalence is often stated by the mnemonic that "lower clocks run slower." This equivalence is observed by noting that an emitted photon (with very well-defined frequency) at a height, h, relative to an absorber (with a very well-defined absorption resonant frequency) at a lower point in a gravitational field will experience an equivalent acceleration as a result of its effective mass by the force of gravity. This acceleration will cause the energy of the photon to increase as it "falls" through the distance h by $\Delta E_{photon} = m_{effective}gh = (hf/c^2)gh$. To the absorber nuclei below the source nuclei, the energy of the photon will thus appear to be greater than needed, so a Doppler shift in the same direction as that of the falling photon will be needed to achieve perfect resonance. To an external observer (who does not recognize gravitational forces), the frequency of the absorber nuclei appears to be running according to a slower clock than that which defines the frequency of the source nuclei.

Pound and Rebka placed an emitter of 14.4125 keV Fe^{57} γ-rays at the top of Harvard University's Jefferson laboratory, h = 22.5 m above absorber nuclei at ground level. They also interchanged the location of source and absorber to see the effect of a photon that must "climb" the height h and therefore loose energy. Electronics and clocks today are so much more precise than they were in 1959 that we can observe that "lower clocks run slower" if they are only separated by a height difference of 1 cm! This makes the concept of a tabletop measure of the equivalence principle very realistic.

PROBLEM

1.3 **a.** Compute the shift in energy caused by the falling photon in the Pound and Rebka experiment and determine the Doppler shift required to achieve resonance.

b. Compute the precision needed to observe a Doppler shift of those photons as they fall through a distance of 1 cm.

Electrostatic Potential

Einstein tried in vain to unify gravitation and electromagnetic fields into a single theory in which no external forces would be needed to explain either. He called this

the unified field theory and regarded his failure to produce the theory the greatest failure of his life. Other theorists today are trying to produce the theory with only partial success. Unfortunately, there appears to be no effective charge on a photon because of its energy. Thus, there is no potential difference between photons that are emitted at a higher scalar electrostatic potential than their absorber nuclei. However, it should be possible to place a limit on the effective charge of a photon by making such a measurement.

PROBLEM

1.4 Assuming that we can arrange a source of 14.4125 keV Fe^{57} γ-rays at an electrostatic potential of 1 MV above the nuclei of an absorber, determine the upper limit on the effective charge on a photon if we have a Mössbauer apparatus capable of determining a Doppler shift to a precision of ±0.001 mm/s.

1.4 PLANE WAVES IN A LOSSY MEDIUM

If a homogeneous medium has an electrical conductivity, σ, then currents can be induced by the electric field intensity of a propagating wave, $\vec{J} = \sigma\vec{E}$. By using the time-harmonic form of field quantities, $\vec{E}(\vec{x}, t) = \vec{E}_s(\vec{x})e^{j\omega t}$ and $\vec{H}(\vec{x}, t) = \vec{H}_s(\vec{x})e^{j\omega t}$ Maxwell's equations become as shown below (Table 1.2).

In the time-harmonic form of Faraday's and Ampere's equations, we can take the curl of both sides to obtain

$$\vec{\nabla}\times\vec{\nabla}\times\vec{E}_S = \vec{\nabla}\cdot\left(\vec{\nabla}\cdot\vec{E}_S\right) - \vec{\nabla}^2\vec{E}_S = -j\omega\mu\vec{\nabla}\times\vec{H}_S = -j\omega\mu\left(\sigma\vec{E}_S + j\omega\varepsilon\vec{E}_S\right)$$
$$\vec{\nabla}^2\vec{E}_S + \left(\omega^2\mu\varepsilon - j\omega\mu\sigma\right)\vec{E}_S = 0 \tag{1.21}$$

and

Table 1.2 Maxwell's equations for a homogeneous conducting medium in the absence of "free" charges and currents

Maxwell's equation	No "free" charges/currents	Harmonic form[a]
$\vec{\nabla}\times\vec{E} = -\partial\vec{B}/\partial t$	$\vec{\nabla}\times\vec{E} = -\mu\partial\vec{H}/\partial t$	$\vec{\nabla}\times\vec{E}_S = -j\omega\mu\vec{H}_S$
$\vec{\nabla}\times\vec{H} = \vec{J} + \partial\vec{D}/\partial t$	$\vec{\nabla}\times\vec{H} = \sigma\vec{E} + \varepsilon\partial\vec{E}/\partial t$	$\vec{\nabla}\times\vec{H}_S = \sigma\vec{E}_S + j\omega\varepsilon\vec{E}_S$
$\vec{\nabla}\cdot\vec{D} = \rho_V$	$\vec{\nabla}\cdot\vec{E} = 0$	$\vec{\nabla}\cdot\vec{E}_S = 0$
$\vec{\nabla}\cdot\vec{B} = 0$	$\vec{\nabla}\cdot\vec{H} = 0$	$\vec{\nabla}\cdot\vec{H}_S = 0$

[a] Math and physics books use the time convention $e^{-i\omega t}$ so the harmonic forms have different signs ($j\rightarrow -i$).

$$\vec{\nabla}\times\vec{\nabla}\times\vec{H}_S=\vec{\nabla}\left(\vec{\nabla}\cdot\vec{H}_S\right)-\vec{\nabla}^2\vec{H}_S=\sigma\vec{\nabla}\times\vec{E}_S+j\omega\varepsilon\vec{\nabla}\times\vec{E}_S=-j\omega\mu\sigma\vec{H}_S+\omega^2\mu\varepsilon\vec{H}_S$$

$$\vec{\nabla}^2\vec{H}_S+\left(\omega^2\mu\varepsilon-j\omega\mu\sigma\right)\vec{H}_S=0 \tag{1.22}$$

Equations 1.21 and 1.22 are both of the vector Helmholtz form:

$$\vec{\nabla}^2\vec{E}_S+k^2\vec{E}_S=0 \text{ with } k^2=\omega^2\mu\varepsilon(1-j\sigma/\omega\varepsilon) \tag{1.23}$$

$$\vec{\nabla}^2\vec{H}_S+k^2\vec{H}_S=0 \text{ with } k^2=\omega^2\mu\varepsilon(1-j\sigma/\omega\varepsilon) \tag{1.24}$$

If the fields are written in terms of their Cartesian components, Equations 1.23 and 1.24 represent six second-order, linear, homogeneous PDEs in a form we have already solved. The solutions for each of the x_i components are

$$\begin{bmatrix}E_i(\vec{x},t)\\H_i(\vec{x},t)\end{bmatrix}=\begin{bmatrix}E_{0,i}\\H_{0,i}\end{bmatrix}e^{-j(k_i x_i-\omega t)} \tag{1.25a}$$

$$\begin{bmatrix}\vec{E}(\vec{x},t)\\\vec{H}(\vec{x},t)\end{bmatrix}=\begin{bmatrix}\vec{E}_0\\\vec{H}_0\end{bmatrix}e^{-j(\vec{k}\cdot\vec{x}-\omega t)}, \tag{1.25b}$$

with $\vec{k}=k\hat{a}_k$. These answers are in the same form as our previous answers for TEM[ξ] waves propagating in the $\hat{a}_k$-direction, with the exception that $k^2=\omega^2\mu\varepsilon(1-j\sigma/\omega\varepsilon)$ is a complex number (*if* σ *and* ε *are both real*).[†]

It is traditional in Electrical Engineering to label the real and imaginary parts of the propagation number, k, as

$$k\equiv\beta-j\alpha, \tag{1.26}$$

where both β and α are real numbers. Squaring the number k and equating it to the material properties constants as above,

$$k^2=(\beta-j\alpha)(\beta-j\alpha)=\left(\beta^2-\alpha^2\right)-j(2\alpha\beta)=\left(\omega^2\mu\varepsilon\right)-j(\omega\mu\sigma) \tag{1.27}$$

Solving for the constants, we find

$$\alpha^2=\left(\omega^2\mu\varepsilon/2\right)\left[\sqrt{1+(\sigma/\omega\varepsilon)^2}-1\right] \text{ and } \beta^2=\left(\omega^2\mu\varepsilon/2\right)\left[\sqrt{1+(\sigma/\omega\varepsilon)^2}+1\right] \tag{1.28}$$

[†] μ and ε arise in Equations 1.21 and 1.22 by making the homogeneous, macroscopic approximation that $\vec{B}=\mu\vec{H}$ and $\vec{D}=\varepsilon\vec{E}$. Often, we will use these equations for a *good*, *nonmagnetic* conductor in which there is relatively little polarization due to the electric dipole character of the propagating medium (e.g., copper) so we may use $\mu\approx\mu_0$ and $\varepsilon\approx\varepsilon_0$ in that application. In that case, $k^2\approx\omega^2\mu_0\varepsilon_0(1-j\sigma/\omega\varepsilon_0)$, and we can use a mathematical convenience of defining an effective $\varepsilon_{r,eff}=(1-j\sigma/\omega\varepsilon_0)$, which takes into account the conductivity as if it were part of the permittivity constant. Two warnings for later analysis: (1) we multiplied and divided by ω in factoring out ω^2 so we cannot consider $\varepsilon_{r,eff}(0)$ without remembering that the correct term to consider is $\lim_{\omega\to 0}\omega\varepsilon_{r,eff}(\omega)$, and (2) $\vec{D}=\varepsilon_0\varepsilon_{r,eff}(\omega)\vec{E}$ only insofar as the permittivity contains the conductivity (i.e., $\varepsilon_{r,eff}(\omega)$ is not expressing the alignment of polar molecules).

$$k = \left(\omega\sqrt{\mu\varepsilon}/\sqrt{2}\right)\left[\sqrt{1+(\sigma/\omega\varepsilon)^2}+1\right]^{1/2} - j\left(\omega\sqrt{\mu\varepsilon}/\sqrt{2}\right)\left[\sqrt{1+(\sigma/\omega\varepsilon)^2}-1\right]^{1/2} \quad (1.29)$$

1. For a **non-conducting medium**, $\sigma = 0$ in Equation 1.29, and k reduces to

$$k = \omega\sqrt{\mu\varepsilon} \quad \text{non-conducting} \quad (1.30a)$$

as in the case of plane waves propagating in a pure dielectric medium.

2. For a **weakly conducting medium** in which $x = (\sigma/\omega\varepsilon) << 1$, we can use a series expansion of the square root terms in Equation 1.29 $[1 + x^2]^{1/2} = [1 + (1/2)x^2 - (1 \cdot 1/2 \cdot 4)x^4 + (1 \cdot 1 \cdot 3/2 \cdot 4 \cdot 6)x^6 - \cdots]$ to see

$$k \approx \omega\sqrt{\mu\varepsilon}\,[1 - j\,\sigma/2\omega\varepsilon] \quad \text{weakly conducting} \quad (1.30b)$$

3. For a **strongly conducting medium** in which $x = (\sigma/\omega\varepsilon) >> 1$, we can see

$$k \approx \omega\sqrt{\mu\varepsilon}\left[(1-j)/\sqrt{2}\,\sqrt{\sigma/\omega\varepsilon}\right] \quad \text{strongly conducting} \quad (1.30c)$$

Orienting the Cartesian coordinates such that the z-axis lies in the direction of $\hat{a}_k$,

$$\begin{bmatrix}\vec{E}(\vec{x},t)\\ \vec{H}(\vec{x},t)\end{bmatrix} = \begin{bmatrix}\vec{E}_0\\ \vec{H}_0\end{bmatrix} e^{-\alpha z} e^{-j(\beta z - \omega t)} \quad (1.31)$$

The constant α in the loss term in Equation 1.31 depends on the relative value of $x = (\sigma/\omega\varepsilon)$ to 1. This quantity is often referred to as the ***static loss tangent***:

$$\tan\delta_S = \sigma/\omega\varepsilon \quad (1.32)$$

NOTE The phase velocity of electromagnetic waves in each of these media is $u_p = \omega/\beta$. Thus, $u_p = c/\sqrt{\varepsilon_r}$ for a nonconducting medium, but $u_p = \left(c/\sqrt{\varepsilon_r}\right)\sqrt{2}\sqrt{\omega\varepsilon/\sigma}$ for a strongly conducting medium.

Complex Permittivity

When an electric field is applied to a dielectric material, it orients molecules with electric dipoles in proportion to the size of the electric field. If the applied field oscillates in time (e.g., in an electromagnetic wave), the dipole orientation will try to follow the direction of the applied field. However, the polar molecules being oriented have a mass m that leads to an inertia of the molecule so that it cannot exactly follow the driving frequency in time so that it sometimes lags and can even become completely out of phase with the driving field. Furthermore, the dipoles that oscillate in an external field may lose energy to their neighbors with a damping

coefficient, b, through friction. The result is a set of N per unit volume dipoles that are driven, damped, harmonic oscillators. In Chapter 5, we show how they produce a relative complex permittivity:

$$\tilde{\varepsilon}_r = 1 + \frac{N\alpha e^2/\varepsilon_0 m}{(\omega_0^2 - \omega^2) + j\omega b/m} = \varepsilon_r' - j\varepsilon_r'', \tag{1.33}$$

where ω_0 is a resonant frequency of the polar molecules. The tilde over ε_r reminds us that the permittivity can be a complex quantity at high frequencies. At very high frequencies, the model permits a displacement of a negative plasma of electronic charge relative to its positive atomic cores; at high frequencies, the model includes the additional displacement of ionic charge in individual atoms; at lower frequencies, the traditional orientation of polar molecules give rise to additional permittivity; and, at low frequencies, in conductors and semiconductors, the driving electric field can also displace free electric charges relative to holes in the material to give a complex permittivity that takes into account the conductivity of the material in the form $\varepsilon_{r,eff} = (1 - j\sigma/\omega\varepsilon_0)$, as stated in a previous footnote. The additional effects lead to a behavior that is similar to the orientation of the polar molecules, but the resonances are at different frequencies so that

$$\tilde{\varepsilon}_r = 1 + \sum_{i=1}^{n} \frac{N_i \alpha_i e^2/\varepsilon_0 m}{(\omega_i^2 - \omega^2) + j\omega b/m} = \varepsilon_r' - j\varepsilon_r'' \tag{1.34}$$

Some texts prefer to write

$$\tilde{\varepsilon}_r(\omega) = 1 + \tilde{\chi}_e(\omega) \tag{1.35}$$

where $\tilde{\chi}_e$ is the electric susceptibility,

$$\tilde{\chi}_e(\omega) = \chi_e'(\omega) - j\chi_e''(\omega) \tag{1.36}$$

Many scientists and engineers (e.g., Kramers-Kronig, Debye, Clausius-Mosotti) have contributed to this field so it is a subdiscipline in its own right. Real materials have their own individual characteristics that do not fit a single characteristic set of variations, but each typically has a real and an imaginary part that vary with frequency. The loss mechanisms depend on the ratio of the imaginary and real parts so the ***alternating electric loss tangent*** is defined as

$$\tan\delta_a = \varepsilon''/\varepsilon' \tag{1.37}$$

For materials with conductivity and dielectric losses, the ***effective electric loss tangent*** is

$$\tan\delta_e = \tan\delta_S + \tan\delta_a = \sigma/\omega\varepsilon' + \varepsilon''/\varepsilon' \tag{1.38}$$

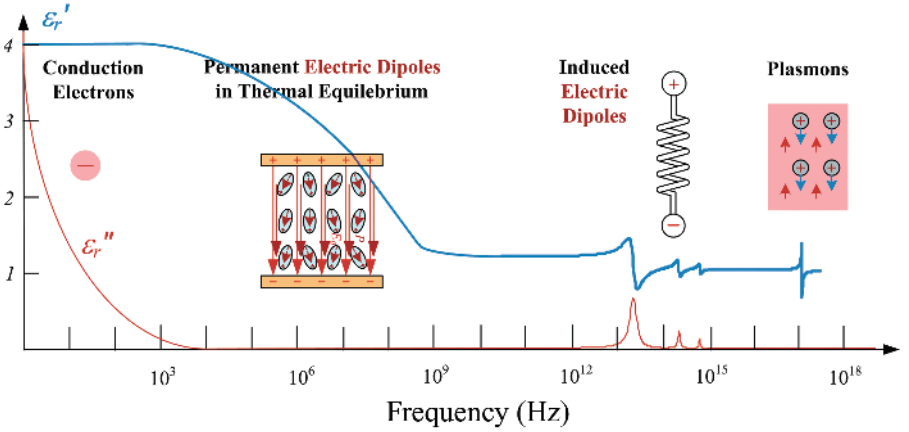

Figure 1.15 Real and imaginary parts of the electric permittivity as a function of frequency for a model dielectric.

We shall hold discussion of the detailed mechanisms that lead to the characteristic resonances in Figure 1.15 to Chapter 5.

Complex Permeability

The macroscopic permeability of many materials classified as diamagnetic, paramagnetic, or antiferromagnetic is nearly the same as free space, $\mu_0 \equiv 4\pi \times 10^{-7}$ H/m or (Ωs/m). Ferromagnetic and ferrimagnetic materials can exhibit much higher permeabilities (sometimes 10^6 times higher) than that of free space. The magnetic dipoles in these materials can be driven in frequency by the magnetic field components in an electromagnetic wave, but, as in the case of the electric dipoles, they have mass and inertia so that they lag behind or are even out of phase with the driving fields. These materials also tend to be lossy, as is seen by their magnetic hysteresis, and the combined effect of dipoles being driven with losses leads to a complex permeability:

$$\tilde{\mu}(\omega) = \mu'(\omega) - j\mu''(\omega) \tag{1.39}$$

Like the case of electric dipoles, the size of the losses depends on the ratio of the complex part of the permeability to the real part, so the ***alternating magnetic loss tangent*** is defined as

$$\tan\delta_m = \mu''/\mu' \tag{1.40}$$

These effects are especially important to the class of ceramic materials called Ferrites that are typically oxides of the metals lithium, magnesium, iron, nickel, zinc,

cadmium, or some of the rare earths. Especially at microwave frequencies, single crystals of these materials exhibit anisotropic magnetic properties and large resistances (they are good insulators), which lead to lower ohmic losses. Ferrites thus appeal to the microwave circuit designer who can incorporate them into devices with resonant characteristics that yield large amplification in preferred directions (especially appealing in antenna design) and can even exhibit preferences for left- or right-hand circularly polarized waves. The science and engineering of ferrites are also the subject of an entire subdiscipline of electrical engineering. It is typical, however, that our homogeneous material approximation fails ($\vec{B} \neq \mu\vec{H}$), and we must write $\vec{B} = \vec{\mu}\vec{H}$ as a tensor operation. This treatment is beyond the scope of this book and will be reserved for an advanced treatment of electromagnetic theory.

Phase Shifts

One of the most important properties of lossy media is that they cause the magnetic field intensity wave propagation to be out of phase with the electric field intensity wave propagation. We can see how this arises by putting the exponential decay forms of fields (Equation 1.31) into the time-harmonic form of Faraday's law:

$$\vec{\nabla} \times \left[\vec{E}_0 e^{-\alpha z} e^{-j\beta z}\right] = -j\omega\mu \vec{H}_0 e^{-\alpha z} e^{-j\beta z} \quad \text{or} \tag{1.41}$$

$$\begin{vmatrix} \hat{a}_x & \hat{a}_y & \hat{a}_z \\ \partial/\partial x & \partial/\partial y & \partial/\partial z \\ E_{0x} e^{-\alpha z} e^{-j\beta z} & 0 & 0 \end{vmatrix} = -j\omega\mu \vec{H}_0 e^{-\alpha z} e^{-j\beta z}, \tag{1.42}$$

where we have chosen the x-axis to lie in the $\vec{E}_0$ direction, so that

$$E_{0x}(-\alpha - j\beta)\hat{a}_y = -j\omega\mu \vec{H}_0 \quad \text{or} \tag{1.43}$$

$$E_{0x} = \frac{j\omega\mu}{(\alpha + j\beta)} H_{0y} = \frac{j\omega\mu(\alpha - j\beta)}{(\alpha + j\beta)(\alpha - j\beta)} H_{0y} = \omega\mu \frac{(\beta + j\alpha)}{(\alpha^2 + \beta^2)} H_{0y} \tag{1.44}$$

The real term in Equation 1.44 shows that part of $\vec{E}_0$ is in phase with (and perpendicular to) $\vec{H}_0$. The imaginary term in Equation 1.44 shows that the other part of $\vec{E}_0$ is perpendicular and leads $\vec{H}_0$ by $\pi/2$.

Conclusions

1. In a conductor, $\vec{H}(x, y, z, t)$ *and* $\vec{E}(x, y, z, t)$ are perpendicular to one another, but $\vec{E}(\vec{x}, t)$ leads $\vec{H}(\vec{x}, t)$ by a phase angle:

$$\varphi = \tan^{-1}(\alpha/\beta) \tag{1.45}$$

2. In a conductor, the relative magnitude of the $\vec{H}(x, y, z, t)$ and $\vec{E}(x, y, z, t)$ fields is

$$\frac{E_x}{H_y} = \tilde{\eta} = \frac{\omega\mu}{\sqrt{\alpha^2 + \beta^2}} e^{j\phi} \tag{1.46}$$

For **nonconducting materials**, we have previously found (Equation 1.30a) that $\alpha = 0$ and $\beta = \omega\sqrt{\mu\varepsilon}$ so that $\varphi = 0$ and $E_x/H_y = \sqrt{\mu/\varepsilon}$, as we previously found in Equation 1.9.

For **weakly conducting materials**, we have found (1.30b) that $\beta - j\alpha \approx \omega\sqrt{\mu\varepsilon}\,[1 - j(\sigma/2\omega\varepsilon)]$ so that $\varphi = \tan^{-1}(\sigma/2\omega\varepsilon)$ and $E_x/H_y \approx \sqrt{\mu/\varepsilon}$, where the term in the parentheses is small. Thus, there is a small phase shift of the electric field intensity to the magnetic field intensity, but the magnitude is about the same as it was for a nonconductor.

For **strongly conducting materials**, we have found (Equation 1.30c) that $\beta - j\alpha \approx \omega\sqrt{\mu\varepsilon}\left[\sqrt{\sigma/\omega\varepsilon}\,(1-j)/\sqrt{2}\right]$ so that $\varphi = \tan^{-1}1/1 = \pi/4\ rad = 45^\circ$ and $E_x/H_y = \omega\mu/\sqrt{\alpha^2 + \beta^2} = \sqrt{\mu/\varepsilon}/\sqrt{(\sigma/\omega\varepsilon)}$, where the term in the parentheses is much larger than 1. Thus, there is a phase shift of 45° and a decrease in the electric field intensity (relative to the magnetic field intensity) over that of a nonconductor.

The decay and phase shift for a strongly conducting medium are shown in Figure 1.16.

Examples

Describe the character of electromagnetic propagation in copper, seawater, and distilled water if σ and ε_r are given as shown in Table 1.3.

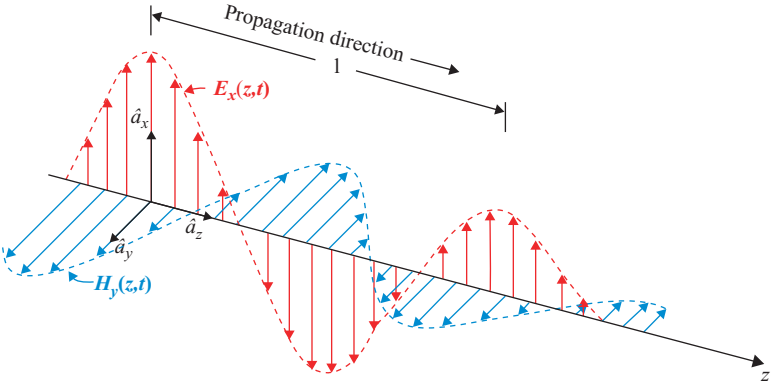

Figure 1.16 Propagation of the electric field intensity and magnetic field intensity of an electromagnetic wave in a strongly conducting material.

Table 1.3 Properties* of selected materials

Material	σ (S/m)	ε_r	$\varepsilon''/\varepsilon'$	μ_r	μ''/μ'
Copper	5.8×10^7	1	0	1	0
Cast iron	1.0×10^6	1	0	60	*
Seawater	4	72	4	1	0
Ferrite (Fe_2O_3)	1.3×10^{-3}	1	0	1000	*
Distilled water	2.0×10^{-4}	80	4×10^{-2}	1	0
Glass	10^{-12}	7	2×10^{-2}	1	0
Resin (FR4)	10^{-15}	4.0	2×10^{-3}	1	0

*Qualifications: Values vary with measurement temperature (typically room temperature), purity, and frequency (typically <10 GHz) of E&M wave. Relative losses of ferromagnetic materials are calculated in Chapter 4.

We have seen from Equation 1.30b and 1.30c that

$$\beta - j\alpha \approx \omega\sqrt{\mu\varepsilon}\,[1 - j\,\sigma/2\omega\varepsilon] \quad \text{weakly conducting}$$
$$\beta - j\alpha \approx \omega\sqrt{\mu\varepsilon}\,\left[\sqrt{\sigma/\omega\varepsilon}\,(1-j)/\sqrt{2}\right] \quad \text{strongly conducting}$$

and that $\tan\delta_s = \sigma/\omega\varepsilon$ is the deciding criterion. Choosing the criteria to be $10^{\pm 2}$,

$\boldsymbol{tan\,\delta}$	$\boldsymbol{\alpha}$	$\boldsymbol{\beta}$	$\boldsymbol{\eta}$	$\boldsymbol{\varphi}$
<0.01	$\sqrt{\mu/\varepsilon}\,\sigma/2$	$\omega\sqrt{\mu\varepsilon}$	$\sqrt{\mu/\varepsilon}$	$\tan^{-1}\sigma/2\omega\varepsilon$
>100	$\sqrt{\omega\sigma\mu}/\sqrt{2}$	$\sqrt{\omega\sigma\mu}/\sqrt{2}$	$\sqrt{\mu/\varepsilon}/\sqrt{\sigma/\omega\varepsilon}$	45°

These criteria lead to a skin depth, δ, magnitude of E_x to H_y, η_{eff}, relative phase angle of $\vec{E}$ to $\vec{H}$, φ, and phase velocity, u_p, of each material based on its material conductivity, as shown in Table 1.4.

Table 1.4 Electromagnetic wave properties in various propagating materials

Material	δ	η_{eff} (V/A)	φ	u_p (m/s)
Copper at 60 Hz	0.85 cm	2.9×10^{-6}	45°	3.2
Copper at 100 MHz	6.6×10^{-3} cm	3.7×10^{-3}	45°	4153
Seawater at 60 Hz	32.5 m	10.1×10^{-3}	45°	1.7×10^8
Seawater at 100 MHz	2.5 cm	14.1	39.3°	7.8×10^7
Distilled water at 60 Hz	4590 m	0.49	44.9°	5.5×10^5
Distilled water at 100 MHz	240 m	19.9	0.013°	5.7×10^7

1.5 DISPERSION AND GROUP VELOCITY

Thus far, we have dealt primarily with monochromatic waves with a definite frequency, ω_0, and the real part of a wave number, $\beta_0 = 2\pi/\lambda_0$, with the possibility that there will be an imaginary part, α_0 that causes waves to decay with propagation distance. We found that these waves have a phase velocity, $u_p = \left(c/\sqrt{\varepsilon_r}\right)$ for a nonconducting medium and $u_p = \left(c/\sqrt{\varepsilon_r}\right)\sqrt{2\omega_0\varepsilon/\sigma}$ for a strongly conducting medium. Thus, waves of definite frequency, ω_0, decay in amplitude with propagation distance, as shown in Figure 1.16, and move with phase velocity less than the speed of light, c, in a vacuum but they do not disperse.

Spread of Frequency Components for a Shaped Pulse

In most applications, electromagnetic waves are produced with a finite spread of frequencies or wavelengths because of the finite duration of a pulse, for example, in the packet shaping of a pulse of light for a fiber-optic transmission line. We can examine the Fourier transform for the packet in time to see the spread of frequencies. If the medium is dispersive (i.e., it is strongly conducting and has a complex permittivity or a complex permeability), the phase velocity of an individual frequency component of the wave will not be the same as those for other frequency components of the wave. In this case, high-frequency components will travel at different phase velocities than low-frequency components, and the pulse will disperse in space and time.

We will begin this characterization by examining the frequency spread of a shaped pulse. We will then examine the group velocity of the pulse through the different phase velocities of its frequency components. Finally, we will characterize the shape of the pulse as it propagates in a dispersive medium.

Frequency Spread of a Shaped Pulse

For simplicity, let us consider the propagation of an amplitude-modulated signal consisting of a carrier frequency signal (of frequency, ω_0) that is modulated by a pulse having a Gaussian distribution shape with time. At $z = 0$, the relative electric field would behave as

$$\vec{E}(0,t) = \vec{E}_0 \cos\omega_0 t\, e^{-t^2/2T_0^2}, \tag{1.47}$$

where T_0 is a measure of the width of the pulse.

The relative electric field intensity given by Equation 1.47 is shown in Figure 1.17. Also shown in this figure is the Gaussian envelope (in green).

The energy of the pulse is proportional to the square of the electric field intensity as

$$\left|\vec{E}(0,t)\right|^2 = \left|\vec{E}_0\right|^2 e^{-t^2/T_0^2} \cos^2\omega_0 t \tag{1.48}$$

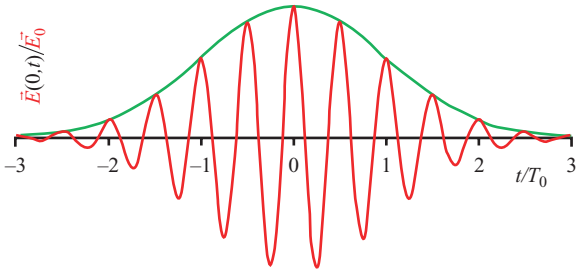

Figure 1.17 Electric field intensity $|\vec{E}(0, t)|/|\vec{E}_0|$ as a function of reduced time, t/T_0, for a Gaussian modulated pulse.

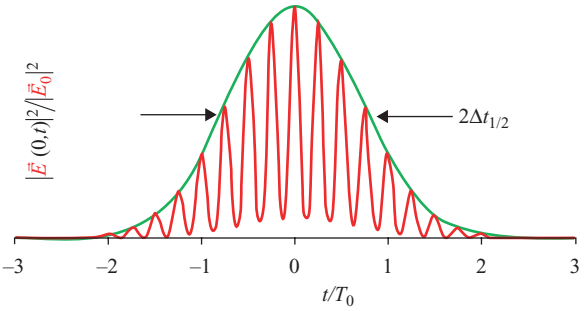

Figure 1.18 Square of the relative transverse electric field intensity, $|\vec{E}(0, t)|^2/|\vec{E}_0|^2$, as a function of reduced time, t/T_0, for a Gaussian modulated pulse.

The relative electric field intensity squared is shown (in red) in Figure 1.18. The envelope is another Gaussian distribution (in green).

Note that the half width of the Gaussian envelope shown in Figure 1.18 occurs at time $t^2 = T_0^2 \ln 0.5$ so the half width at half maximum (HWHM) is

$$\Delta t_{1/2} = \sqrt{0.693}\, T_0 \tag{1.49}$$

Example

The envelope in these figures relative to the carrier frequency is greatly exaggerated for a typical pulse application. For example, a typical optical pulse might have $2T_0 \approx 10^{-10}$ s and $\lambda_0 = 300$ nm ($f_0 = 10^{15}$ Hz) for ultraviolet (UV) light in a fiber-optic cable; thus, $n = c(2T_0)/\lambda_0 \approx 10^5$ cycles under the full width at half maximum (FWHM) of curve 1-18 (vs. ≈6 shown).

The Phasor electric field intensity is thus the real part of $E(0, t) = E_0 e^{-t^2/2T_0^2} e^{j\omega_0 t}$ whose Fourier transform is

$$\tilde{E}(0,\omega) = \int_{-\infty}^{\infty} E(0,t)e^{-j\omega t}\,dt \tag{1.50}$$

$$\text{or} \quad \tilde{E}(0,\omega) = \int_{-\infty}^{\infty} E_0 e^{-t^2/2T_0^2} e^{-j(\omega-\omega_0)t}\,dt \tag{1.51}$$

which can be written

$$\tilde{E}(0,\omega) = 2E_0\int_0^{\infty} e^{-t^2/2T_0^2}\cos(\omega-\omega_0)t\,dt = \sqrt{\pi}E_0 T_0 e^{-(\omega-\omega_0)^2 T_0^2/2} \tag{1.52}$$

Conclusion

The Fourier transform of a Gaussian modulated electric field intensity oscillating at carrier frequency ω_0 in time is another Gaussian in frequency space centered about $\omega = \omega_0$; that is, modulating the pure electromagnetic wave with a single carrier frequency with a Gaussian envelope yields an electromagnetic wave with a distribution of frequencies (also in a Gaussian fashion) about the carrier frequency.

If we express the relative energy of this electric field intensity in frequency space as proportional to

$$\tilde{E}^2(0,\omega) = \pi E_0^2 T_0^2 e^{-(\omega-\omega_0)^2 T_0^2}, \tag{1.53}$$

and we can plot the energy spectrum, as shown in Figure 1.19.

We can see that the energy spectrum falls to 0.5 for $\omega = \omega_0 \pm \sqrt{0.693}/T_0$; that is,

$$\Delta\omega_{1/2} = \sqrt{0.693}/T_0 \tag{1.54}$$

It is interesting to note that the product of Equations 1.49 and 1.54 yields

$$\Delta t_{1/2}\Delta\omega_{1/2} = 0.693 \tag{1.55}$$

We can multiply Equation 1.55 through by $\hbar$ and compare this result with that of the Heisenberg Uncertainty principle:

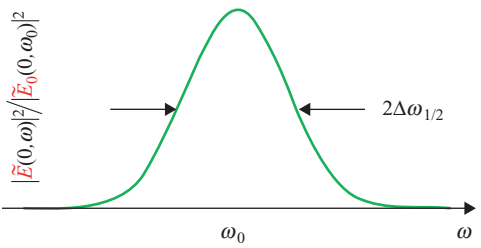

Figure 1.19 Relative energy spectrum, $|\tilde{E}(0,\omega)|^2/|\tilde{E}(0,\omega_0)|^2$, of a Gaussian modulated pulse of a pure electromagnetic wave, with carrier frequency ω_0 as a function of frequency ω.

$$\Delta t_{1/2}\hbar\Delta\omega_{1/2} \geq 0.500\,\hbar \tag{1.56}$$

to see that the uncertainty principle is a mathematical statement about the shape of pulses and their Fourier transforms; that is, for Gaussian modulated pulses, the uncertainty in time (HWHM of the energy spectrum) times the uncertainty in frequency (HWHM in energy divided by $\hbar$) is a constant (0.693).

Example

For the example above, with $\lambda_0 = 300$ nm, $\omega_0 = 2\pi \times 10^{15}$ Hz, and $\Delta t_{1/2} = \sqrt{0.693}\,T_0 = \sqrt{0.693}\,10^{-10}\text{s}/2$, $\Delta\omega_{1/2} = 1.66 \times 10^{10}\ \text{s}^{-1}$ and $\Delta\omega_{1/2}/\omega_0 = 2.65 \times 10^{-6}$.

We can conclude that a Gaussian-modulated electromagnetic wave will have components of frequency about the carrier frequency in a Gaussian distribution and that the width of the pulse in time will govern the width of the pulse in frequency space, according to Equation 1.55. For long pulses in time the width of the frequency, Gaussian will be very narrow; we can even take the $\lim \Delta t_{1/2} \to \infty$ to see that the Gaussian will become a delta function (i.e., only one frequency at ω_0). However, for very short pulses of an electromagnetic wave in time, we can see from Equation 1.55 that the frequency distribution will be very broad; that is, there will be a broad distribution of frequency components in the resulting frequency Gaussian.

If the medium in which the pulse is propagating has a dispersive character, that is, the phase velocity depends positively on the frequency of the wave, then the Gaussian distribution will spread out as the wave propagates because the higher frequency components will move with a higher velocity from the lower frequency components. Almost all media exhibit this property so it is called ***normal dispersion***. In rare cases, the Gaussian distribution will narrow as the wave propagates because the higher frequency components move with a lower velocity for the lower frequency components. Pulses that exhibit this property in a medium are said to have ***anomalous dispersion***. In either case, we need to define a new velocity of propagation of the group of wave components that constitute a pulse, which we will call u_g, the group velocity.

Group Velocity

As mentioned above, we found that electromagnetic waves traveling in a medium have a phase velocity, $u_p = c/\sqrt{\varepsilon_r}$ if the medium is nonconducting and $u_p = \left(c/\sqrt{\varepsilon_r}\right)\sqrt{2\omega_0\varepsilon/\sigma}$ if the medium is strongly conducting. We have also shown that information pulses shaped by a Gaussian envelope in time are described as a Gaussian distribution of frequencies. As shown in Figure 1.15, dielectrics generally exhibit decreasing permittivity with frequency (ignoring the resonances, which are discussed in Chapter 5) so the higher frequency components of those pulses will travel with higher phase velocity and the amplitude of each Fourier component will decay as $e^{-\alpha z} = e^{-\sqrt{\mu/\varepsilon}\,\sigma z/2}$, where σ is very small so they will separate in time (i.e.,

they will disperse) but will not decay very much with distance. In *good* conductors, we observed in Table 1.4 that phase velocity is frequency dependent, and, in addition, the Fourier components will decay in amplitude, with z as $e^{-\alpha z} = e^{-\sqrt{\mu/\varepsilon}\sqrt{2\omega\sigma}\, z/2}$, where σ is relatively large so the frequency components will move with different phase velocities (i.e., they will disperse) and they will decay rapidly with distance.

We thus need a new velocity to define the "average" velocity of a group of plane wave components with different frequencies. To simplify our understanding of the new definition, we will begin with only ***two*** plane waves with different frequencies $\omega + \Delta\omega/2$ and $\omega - \Delta\omega/2$ that differ in frequency by a small amount, $\Delta\omega$, and we will take the limit as $\Delta\omega \to 0$. We will then extend the argument to include additional different frequencies (always taking the limit as $\Delta\omega \to 0$) and thereby build up a continuum of frequencies in a pulse.

Figure 1.20 shows the linear combination of two plane waves of equal amplitude but slightly different frequencies, $\omega + \Delta\omega/2$ and $\omega - \Delta\omega/2$, in time. We have seen that the real part of the propagation constant, β, also depends on frequency in any conductor (good or bad) so there will be a corresponding $\beta + \Delta\beta/2$ and $\beta - \Delta\beta/2$ for each of the two waves.

The mathematical sum of the two electric field waves is given by the linear combination

$$\vec{E}_{total}(\vec{x}, t) = \vec{E}_{01}(z)e^{-\alpha z}\, e^{j\left[\left(\beta+\frac{\Delta\beta}{2}\right)z-\left(\omega+\frac{\Delta\omega}{2}\right)t\right]} + \vec{E}_{02}(z)e^{-\alpha z}\, e^{j\left[\left(\beta-\frac{\Delta\beta}{2}\right)z-\left(\omega-\frac{\Delta\omega}{2}\right)t\right]} \qquad (1.57)$$

NOTE In Equation 1.57, we have assumed that the two waves are decaying with z by the same decay constant, α. In a rigorous treatment, we would have to take this into account for strong conductors by considering two different values of α but would eventually take the limit as the two values of α approached one another and the outcome would be the same.

If the two waves have equal amplitude, $\vec{E}_0(z)$, then the real part of Equation 1.57 may be written as

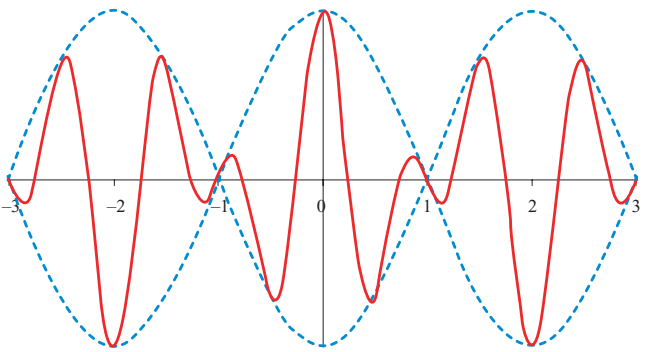

Figure 1.20 Sum of two plane waves with equal amplitude but different base frequency ω by $\Delta\omega$.

$$\begin{aligned}&\mathrm{Re}\,\vec{E}_{total}(\vec{x},t)\\&=\vec{E}_0(z)e^{-\alpha z}\left\{\cos\left[\left(\beta+\frac{\Delta\beta}{2}\right)z-\left(\omega+\frac{\Delta\omega}{2}\right)t\right]+\cos\left[\left(\beta-\frac{\Delta\beta}{2}\right)z-\left(\omega-\frac{\Delta\omega}{2}\right)t\right]\right\},\end{aligned}$$

and, by using the mathematical identity for the product of cosines,

$$\mathrm{Re}\,\vec{E}_{total}(\vec{x},t)=2\vec{E}_0(z)e^{-\alpha z}\cos(\Delta\beta z-\Delta\omega t)\cos(\beta z-\omega t) \tag{1.58}$$

Assuming $\Delta\omega << \omega$, the term $\cos(\Delta\beta z - \Delta\omega t)$ in Equation 1.58 describes the envelope of the base plane wave shown in Figure 1.19. The velocity of the envelope is called the "group velocity," u_g. We can find the velocity of the envelope by considering a point of constant envelope amplitude, $(\Delta\beta z - \Delta\omega t)$ = constant, and then take the derivative with respect to time to obtain $u_g = dz/dt = \Delta\omega/\Delta\beta$, and, taking the limit as $\Delta\omega \to 0$,

$$u_g=\frac{dz}{dt}=\lim_{\Delta\omega\to 0}\frac{\Delta\omega}{\Delta\beta}=\frac{1}{d\beta/d\omega}=\left.\frac{d\omega}{d\beta}\right|_{avg} \tag{1.59}$$

The group velocity, u_g, of the waves is thus the derivative of the ω versus β curve evaluated at the point ω. The group velocity is in contrast to the phase velocity of the waves, u_p, which is just the ratio of ω to β.

If the group velocity of two waves that are infinitesimally close in frequency is less than the phase velocity, we call the propagation and the dispersion normal. If the group velocity of the two waves equals the phase velocity, there will be no difference in their speed and there will be no dispersion. If the group velocity is greater than the phase velocity, the propagation and dispersion are said to be anomalous.

$$\begin{array}{ll}u_g < u_p & \text{Normal dispersion}\\ u_g = u_p & \text{No dispersion}\\ u_g > u_p & \text{Anomalous dispersion}\end{array} \tag{1.60}$$

Shape of the Pulse

For the pulse modulated by a Gaussian distribution above, a relatively long pulse will produce a relatively narrow frequency band. By comparison, β will be a slowly varying function of ω so we can expand β in a Taylor's series about the carrier frequency ω_0 and keep only the first three terms:

$$\beta(\omega)\approx\beta(\omega_0)+(\omega-\omega_0)\left.\frac{d\beta}{d\omega}\right|_{\omega_0}+\frac{1}{2}(\omega-\omega_0)^2\left.\frac{d^2\beta}{d\omega^2}\right|_{\omega_0} \tag{1.61}$$

Substituting this approximation into the inverse Fourier transform,

$$\vec{E}(z,t) = \frac{1}{2\pi}\int_{-\infty}^{\infty} \tilde{E}(z,\omega)e^{j\omega t}\,d\omega$$
$$= \frac{1}{2\pi}\int_{-\infty}^{\infty} \tilde{E}(0,\omega)e^{-(\alpha+j\beta)z}\,e^{j\omega t}\,d\omega \tag{1.62}$$

$$\vec{E}(z,t) \approx \frac{1}{2\pi}\int_{-\infty}^{\infty} \tilde{E}(0,\omega')e^{-\alpha z}\,e^{-j\beta(\omega_0)z}\,e^{-j\omega'\beta' z}\,e^{-j\omega'^2\beta'' z}\,e^{j\omega_0 t}\,d\omega'$$
$$\text{where } \omega' = (\omega-\omega_0),\ \beta' = (d\beta/d\omega)|_{\omega_0},\ \textit{and}\ \beta'' = \left(d^2\beta/d\omega^2\right)_{\omega_0} \tag{1.63}$$

If we now employ Equation 1.53 $\tilde{E}^2(0,\omega) = \pi E_0^2 T_0^2 e^{-(\omega-\omega_0)^2 T_0^2}$ in Equation 1.63, we obtain

$$\vec{E}(z,t) \approx \frac{\sqrt{\pi}\vec{E}_0 T_0}{2\pi}\int_{-\infty}^{\infty} e^{-\frac{\omega'^2 T_0^2}{2}}\,e^{-\alpha z}\,e^{-j\beta(\omega_0)z}\,e^{-j\omega'\beta' z}\,e^{-j\omega'^2\beta'' z/2}\,e^{j\omega_0 t}\,d\omega' \tag{1.64}$$

Taking the terms that are independent of ω' out of the integral, we get

$$\vec{E}(z,t) \approx \frac{\vec{E}_0 T_0}{2\sqrt{\pi}}e^{-\alpha z}e^{-j[\beta(\omega_0)z-\omega_0 t]}\int_{-\infty}^{\infty} e^{-\omega'^2\frac{T_0^2}{2}}e^{-j\omega'^2\frac{\beta'' z}{2}}e^{j\omega'(t-\beta' z)}d\omega' \tag{1.65}$$

$$\text{or}\quad \vec{E}(z,t) \approx \frac{\vec{E}_0}{\sqrt{1+j\beta'' z/T_0^2}}e^{-\alpha z-j[\beta(\omega_0)t-\omega_0 t]}\,e^{-\left\{(t-\beta' z)^2\left[1-j\beta'' z/T_0^2\right]\right\}/\left(T_0^2+(\beta'' z/T_0)^2\right)} \tag{1.66}$$

Now, if we let

$$t_0 = \beta' z = \frac{z}{u_g|_{\omega_0}} = \text{group delay at } \omega_0 \tag{1.67}$$

$$\text{and}\quad S = \beta'' z/T_0 \tag{1.68}$$

$$\vec{E}(z,t) \approx \frac{\vec{E}_0}{\sqrt{1+jS/T_0}}e^{-\alpha z-j[\beta(\omega_0)t-\omega_0 t]}\,e^{-\left\{(t-t_0)^2[1-jS/T_0]\right\}/\left(T_0^2+S^2\right)} \tag{1.69}$$

Equation 1.66 or 1.69 may be interpreted as a plane propagating in the z-direction at the carrier frequency modified by a pulse envelope:

$$\text{Envelope} = e^{-(t-t_0)^2/T_0^2\sigma^2}\Big/\sigma \tag{1.70a}$$

where

$$\sigma = \sqrt{1+jS/T_0} \tag{1.70b}$$

at $z = 0$, $t_0 = 0$ and $S = 0$ so we can see that Equation 1.70 reduces to Equation 1.48, our initial Gaussian-shaped pulse. As the pulse propagates to some positive value

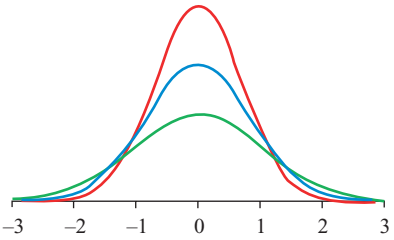

Figure 1.21 Amplitude of the Gaussian-shaped pulse envelope for a carrier wave propagating along the z-axis and centered at $z_0 = 0$, $z_1 = T_0/\beta''$, and $z_2 = 2T_0/\beta''$ for corresponding times $t_0 = 0$, $t_1 = (\beta'/\beta'')T_0$, and $t_2 = 2(\beta'/\beta'')T_0$.

of z, Equation 1.70 shows that the initial pulse is decreasing in amplitude, changing in phase, and becoming broader. The envelope of the pulse is shown in Figure 1.21.

In Figure 1.21, we can interpret the horizontal axis as corresponding either to the width of the pulse in physical space along the z-axis or to the width of the pulse in time. The height is the amplitude of the envelope that constrains the electric field oscillating at the carrier frequency. We can see from Figure 1.21 that the amplitude is quickly dying with propagation distance (or time) and that the pulse width is slowly increasing with propagation distance (or time).

For a plane wave propagating in a uniform material medium, we can define a phase refractive index, n, for the phase velocity relative to the speed of light in a vacuum by

$$u_p\big|_{\omega_0} = \omega_0/\beta(\omega_0) = c/n \tag{1.71a}$$

and a group refractive index, N, by

$$u_g\big|_{\omega_0} = (d\omega/d\beta)_{\omega_0} = 1/\beta' = c/N \tag{1.71b}$$

If we expand n as a Taylor series in frequency about ω_0, we can write $n \approx n(\omega_0) + (\omega - \omega_0)dn/d\omega$ and, using $(\omega/2\pi)\lambda_0 = c$, we can see

$$\frac{dn}{d\omega} = \frac{dn}{d\lambda_0}\frac{d\lambda_0}{d\omega} = \frac{dn}{d\lambda_0}\left(-\frac{2\pi c}{\omega^2}\right) \tag{1.72a}$$

so that

$$\frac{d\beta}{d\omega} = \frac{1}{c}\left(n - \lambda_0\frac{dn}{d\lambda_0}\right) \tag{1.72b}$$

and thus

$$N = n - \lambda_0\, dn/d\lambda_0 \tag{1.72c}$$

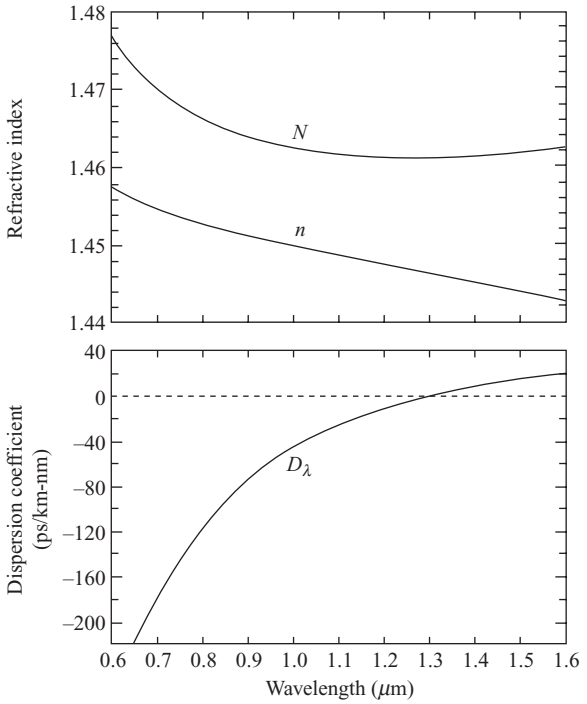

Figure 1.22 Group refractive index, N, phase refractive index, n, and dispersion coefficient, D_λ, for fused silica as a function of wavelength.

We can also find $S = \beta'' z/T_0$ in terms of the index of refraction by taking another derivative of $\dfrac{d\beta}{d\omega} = \dfrac{1}{c}\left(n - \lambda_0 \dfrac{dn}{d\lambda_0}\right)$; $\beta'' = \dfrac{d}{d\omega}\left(\dfrac{d\beta}{d\omega}\right) = \dfrac{d}{d\lambda_0}\left[\dfrac{1}{c}\left(n - \lambda_0 \dfrac{dn}{d\lambda_0}\right)\right]\dfrac{d\lambda_0}{d\omega}$ or

$$S = (T_0 c/2\pi) D_\lambda \, z \tag{1.73}$$

where D_λ is called the dispersion coefficient.

The group refractive index, the phase refractive index, and the dispersion coefficient for fused silica are shown plotted in Figure 1.22.

Note that for a nonmagnetic medium, the phase index of refraction is the same as the square root of the relative permittivity ε_r. From Figure 1.20, we can see that the group refractive index (the relative velocity of a pulse envelope) is constant for visible wavelengths above 1000 nm but depends on wavelength below 1000 nm (visible light is between 400 and 700 nm).

PROBLEM

1.5 Suppose we pulse shape a 3×10^{14} Hz carrier frequency with a Gaussian envelope with $T_0 = 10^{-10}$ s at 1 GHz and put it into a fused silica transmission line.

a. How many peaks of the electric field intensity vector are under the FWHM of the Gaussian envelope?

b. What is the physical distance between two pulses near the insertion point?

c. How far can pulses propagate until their envelope amplitudes overlap by more than 50%?

1.6 POWER AND ENERGY PROPAGATION

In 1884, the English physicist John H. Poynting developed the theory of power transmission in electromagnetic waves through the use of the cross product of the electric field intensity and magnetic field intensity, which for a TEM wave, is in the direction of propagation. The label for the quantity varies with author (sometimes expressed as $\vec{\mathcal{S}}$), but we shall use the script letter $\vec{\mathcal{P}}$ in Poynting's honor:

$$\vec{\mathcal{P}} = \vec{E}\times\vec{H} \tag{1.74}$$

INTERPRETATION We can see that $\vec{\mathcal{P}}$ is in the direction of propagation with the help of Figure 1.23 by using the right-hand rule to find $\vec{E}\times\vec{H}$. We may use Maxwell's equations from Table 1.2 to find the magnitude of $\vec{\mathcal{P}}$.

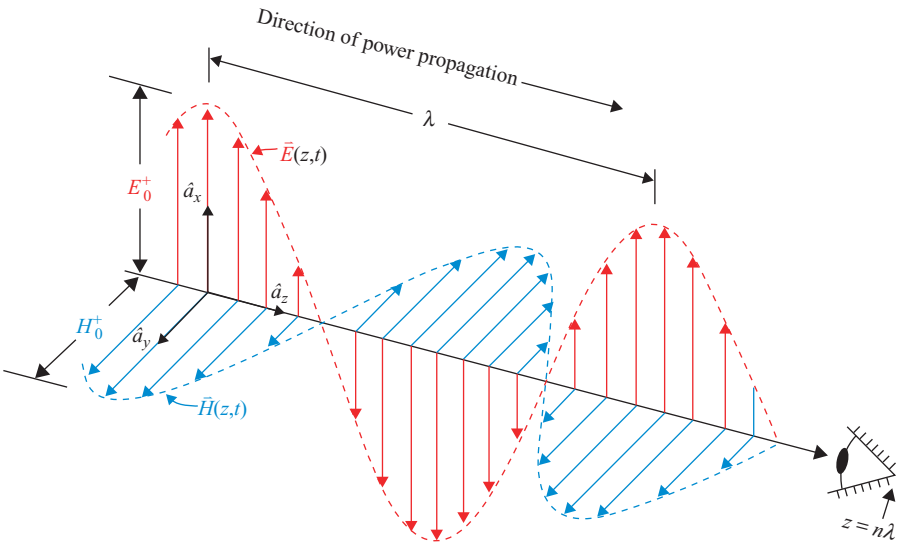

Figure 1.23 Direction of $\vec{\mathcal{P}}$ relative to the electric field intensity and magnetic field intensity.

In Cartesian coordinates, we can show by brute force that

$$\vec{\nabla}\cdot\left(\vec{E}\times\vec{H}\right)=\vec{H}\cdot\left(\vec{\nabla}\times\vec{E}\right)-\vec{E}\cdot\left(\vec{\nabla}\times\vec{H}\right) \tag{1.75}$$

One of our fundamental theorems is that the choice of coordinate system cannot influence the outcome of a physical principle, so we can assert that Equation 1.75 is valid in any coordinate system.

Thus,

$$\vec{\nabla}\cdot\left(\vec{E}\times\vec{H}\right)=\vec{H}\cdot\left(-\partial\vec{B}/\partial t\right)-\vec{E}\cdot\left(\vec{J}+\partial\vec{D}/\partial t\right), \tag{1.76}$$

and, by using the constitutive relations $\vec{B}=\mu\vec{H}$, $\vec{D}=\varepsilon\vec{E}$, and $\vec{J}=\sigma\vec{E}$ for a linear, isotropic medium,

$$\vec{\nabla}\cdot\left(\vec{E}\times\vec{H}\right)=-\mu\frac{\partial}{\partial t}\left(\frac{1}{2}\vec{H}\cdot\vec{H}\right)-\sigma\left(\vec{E}\cdot\vec{E}\right)-\varepsilon\frac{\partial}{\partial t}\left(\frac{1}{2}\vec{E}\cdot\vec{E}\right) \tag{1.77}$$

If we now use the Divergence Theorem to integrate Equation 1.77 over a surface S that surrounds volume V,

$$\oint_S\left(\vec{E}\times\vec{H}\right)\cdot d\vec{\sigma}=-\frac{\partial}{\partial t}\left(\iiint_V\frac{1}{2}\mu H^2 d^3x\right)-\iiint_V\sigma E^2 d^3x-\frac{\partial}{\partial t}\left(\iiint_V\frac{1}{2}\varepsilon E^2 d^3x\right) \tag{1.78}$$

In Equation 1.78, we can recognize the terms $\mu H^2/2$ and $\varepsilon E^2/2$ as the energy density of an electromagnetic field. In addition, we can recognize the term $\sigma E^2 = J^2/\sigma = I^2/\sigma A^2$, where I/A is the current per unit area (the current density) so we can express $-\iiint_V(1/\sigma A)\left(I^2/A\right)d^3x=-\int_L I^2(\rho/A)\,dx=-I^2R$ as the energy loss due to current, I, in a resistor, R, formed by the conducting material in volume V.

We can see that the left-hand side of Equation 1.78 is the integral of the Poynting vector, $\vec{\mathcal{P}}$, over the surface, S, that encloses the volume V. The right-hand side of Equation 1.78 is the negative time rate of change of energy (in the electric field, the magnetic field, and the ohmic conductor) in the volume V. Time rate of change is power so Equation 1.78 states in words

> *"The energy flowing out of volume V through its surface S, is the integral over the surface S of the Poynting vector."*

We can thus interpret the Poynting vector, $\vec{\mathcal{P}}$, as the instantaneous power per unit area flowing across a surface. The units of $\vec{\mathcal{P}}$ should thus be *Watts* per unit area, as we can confirm by $\vec{E}\times\vec{H}$, which would be in $(V/m)(A/m)$.

Time Average Power Density

Figure 1.23 shows that $\vec{\mathcal{P}}$ is a time-dependent quantity for the special case of TEM waves propagating in a lossless medium. In the case of a lossy medium, we have

seen from Figure 1.16 that there is a phase shift between the magnetic field intensity and electric field intensity, and Equation 1.43 showed that, in the general case of TEM waves with no finite boundary conditions (in otherwise free space), $\vec{E}$ and $\vec{H}$ are related by the complex propagation constant $\tilde{k} = \beta - j\alpha$ as $(\beta - j\alpha)\hat{a}_k \times \vec{E}_0 = \omega\mu\vec{H}_0$ or

$$\vec{H}_0 = [(\beta - j\alpha)/\omega\mu]\hat{a}_k \times \vec{E}_0 = (1/\tilde{\eta})\hat{a}_k \times \vec{E}_0 \tag{1.79}$$

where

$$\tilde{\eta} \equiv \omega\mu/(\beta - j\alpha) = |\tilde{\eta}|e^{j\theta_\eta} \tag{1.80}$$

is a complex quantity (signified by the tilde) called the ***complex intrinsic impedance***.

To evaluate $\vec{\mathcal{P}}$, we can express the electric and magnetic field intensity as

$$\vec{E}(z,t) = \mathrm{Re}\left[\vec{E}_S(z)e^{j\omega t}\right] = \hat{a}_x E_0 e^{-\alpha z}\,\mathrm{Re}\left[e^{j(\beta z - \omega t)}\right] = \hat{a}_x E_0 e^{-\alpha z}\cos(\beta z - \omega t)$$

and

$$\vec{H}(z,t) = \mathrm{Re}\left[(E_0/|\tilde{\eta}|)e^{-\alpha z}\,e^{j(\beta z - \omega t)}\,e^{-j\theta_\eta}\right]\hat{a}_y = \hat{a}_y(E_0/|\tilde{\eta}|)e^{-\alpha z}\cos(\beta z - \omega t - \theta_\eta)$$

to write the Poynting vector as

$$\vec{\mathcal{P}}(z,t) = \vec{E} \times \vec{H} = \left(E_0^2/|\tilde{\eta}|\right)e^{-2\alpha z}\cos(\beta z - \omega t)\cos(\beta z - \omega t - \theta_\eta)\vec{a}_z \tag{1.81}$$

or with a mathematical identity for the cosine

$$\vec{\mathcal{P}}(z,t) = \left(E_0^2/|\tilde{\eta}|\right)e^{-2\alpha z}(1/2)[\cos\theta_\eta + \cos(2\beta z - 2\omega t - \theta_\eta)]\hat{a}_z \tag{1.82}$$

We can see that this quantity varies with time with a frequency $2\omega = 4\pi/T$ so, if we take the time average, evaluated at a particular point z, by averaging over an integer number of n cycles,

$$\vec{\mathcal{P}}_{Avg} = (1/nT)\int_0^{nT}\left(E_0^2/|\tilde{\eta}|\right)e^{-2\alpha z}(1/2)[\cos\theta_\eta + \cos(2\beta z - 2\omega t - \theta_\eta)]\hat{a}_z\,dt \tag{1.83}$$

or

$$\vec{\mathcal{P}}_{Avg} = \left(E_0^2/2|\tilde{\eta}|\right)e^{-2\alpha z}\cos\theta_\eta\,\hat{a}_z\left(W/m^2\right) \tag{1.84}$$

NOTE Equation 1.84 is equivalent to

$$\vec{\mathcal{P}}_{Avg} = (1/2)\,\mathrm{Re}\left[\vec{E} \times \vec{H}^*\right]. \tag{1.85}$$

PROBLEM

1.6 Compute $\vec{E} \times \vec{H}^*$ for E&M fields in a lossy medium to show that Equations 1.84 and 1.85 yield the same values.

1.7 MOMENTUM PROPAGATION

We can see that an electromagnetic field in the form of light has momentum by observing the effect of radiation pressure on a balanced vane that has a silver reflecting surface on one side and a black absorbing surface on the other. Such a device is called a Crooke's radiometer and is shown in Figure 1.24.

Normally, the rotation of the vane is explained by the photon concept of light in which photons are merely absorbed by the black surface, while photons are reflected by the silver surface. It is argued that the momentum change for the absorbed photon is thus half as much as the momentum change for the reflected photon and thus greater pressure is applied to the silver side of the vane than to the black side. Unless the glass bulb is highly evacuated, the molecules on the dark surface cause heating of the residual gas in the bulb, which in turn exerts a greater pressure on the black surface, causing the vane to turn in the wrong direction.

Electromagnetic pressure was predicted by James Maxwell in 1899 and demonstrated experimentally by Peter Lebedev. NASA has even proposed to use the pressure of sunlight to accelerate a solar sail-ship fitted with a huge silver sail. A variation of the space sail has been proposed in the form of a magnetic sail (magsail) which would cause a superconducting current loop to be oriented normal to charged particles in the solar wind to impart momentum and thus accelerate the spacecraft in the direction of the wind.

Some scientists, including Lord Kelvin and Helmholtz in 1871, have proposed[4] a "radio-panspermia theory" that radiation pressure could be the propulsion system

Figure 1.24 Crooke's radiometer.

that transported spores and bacteria through interstellar space to populate the first life forms on earth.[5]

ENDNOTES

1. E. G. Harris, Paul G. Huray, F. E. Obenshain, J. O. Thompson, and R. A. Villecco, "Experimental Test of Weyl's Gauge-Invariant Geometry," *Physical Review* D 7, no. 8 (April 1973): 15.
2. R. V. Pound, and G. A. Rebka Jr., "Gravitational Red-Shift in Nuclear Resonance," *Physical Review Letters* 3, no. 9 (1959): 439–41.
3. Hans C. Ohanian, *Gravitation and Spacetime* (New York: W. W. Norton, 1976).
4. S. Arrhenius, "The Propagation of Life in Space," *Die Umschau* 7 (1903): 481.
5. A website on the Panspermia theory can be found at http://www.panspermia.org/.